THE LANCET
Planetary Health

Supplementary appendix 1

This appendix formed part of the original submission and has been peer reviewed. We post it as supplied by the authors.

Supplement to: Iungman T, Khomenko S, Barboza EP. The impact of urban configuration types on urban heat islands, air pollution, CO2 emissions, and mortality in Europe: a data science approach. *Lancet Planet Health* 2024; **8:** e489–505.

The impact of urban configuration types on urban heat islands, air pollution, CO_2 emissions and mortality in Europe: a data science approach

Tamara Iungman MPH [a,b,c] *, Sasha Khomenko PhD [a,b,c] *, Evelise Pereira Barboza MPH [a,b,c], Marta Cirach MSc [a,b,c], Karen Gonçalves PhD [a,b,c], Paula Petrone PhD [a,b,c], Thilo Erbertseder PhD [d], Prof. Hannes Taubenböck PhD [d,e], TC Chakraborty PhD [f], Mark Nieuwenhuijsen PhD [a,b,c] **

* First co-authors
** Corresponding author

[a] *Institute for Global Health (ISGlobal), Barcelona, Spain*
[b] *Department of Experimental and Health Sciences, Universitat Pompeu Fabra (UPF), Barcelona, Spain*
[c] *CIBER Epidemiología y Salud Pública (CIBERESP), Madrid, Spain*
[d] *German Aerospace Center (DLR), Earth Observation Center (EOC), Oberpfaffenhofen, Germany*
[e] *Institute for Geography and Geology, Julius-Maximilians-Universität Würzburg, Würzburg, Germany*
[f] *Atmospheric, Climate, & Earth Sciences Division, Pacific Northwest National Laboratory, Richland, WA, USA*

Supplementary material

A) European cities dataset.
B) Division of cities into rings.
C) Local Climate Zones (LCZs) classification.
D) Open Street Map (OSM) road classification.
E) Motorized traffic flows.
F) Surface Urban Heat Island (SUHI).
G) Tropospheric Nitrogen Dioxide (NO_2).
H) CO_2 emissions.
I) Main analysis.
J) Validation of the NO_2 exposure and CO_2 emissions variables.
K) Sensitivity analyses.
L) Mortality rates.

A) **European cities dataset.**

Our analysis focused on European cities listed in the Urban Audit dataset 2018 (1), which follows the city definition by the Organization for Economic Cooperation and Development - European Commission (OECD-EC), based on population density and local administrative boundaries (2). The original dataset encompasses 980 cities across 31 European countries (EU27, United Kingdom (UK), Norway, Switzerland and Iceland). We excluded Saint Denis (Réunion) and Fort-de-France (Martinique) due to their location outside of the European study area. Since the City of London is primarily an economic hub rather than a residential area (with only 8,600 inhabitants in 2021), we opted to include Greater London instead and excluded the 32 London boroughs encompassed within the Greater London area to avoid double-counting (3). Overall, we considered 946 European cities for the analysis. We collected all data at 250m x 250m grid cell resolution based on the Global Human Settlement Layer (GHSL) population dataset for 2015 (4), following the same data collection procedure as in our previous studies (5–8). Given that the GHSL had population misallocations into non-residential areas and we were interested in describing populated areas in terms of urban configuration and exposures, we adjusted the GHSL layer to include only grid cells overlapping with residential areas from the Urban Atlas and redistributed the misallocated population into the remaining grid cells proportionally based on the GHSL population density (6,7). In total, our dataset included n = 825,148 grid cells.

B) **Division of cities into rings.**

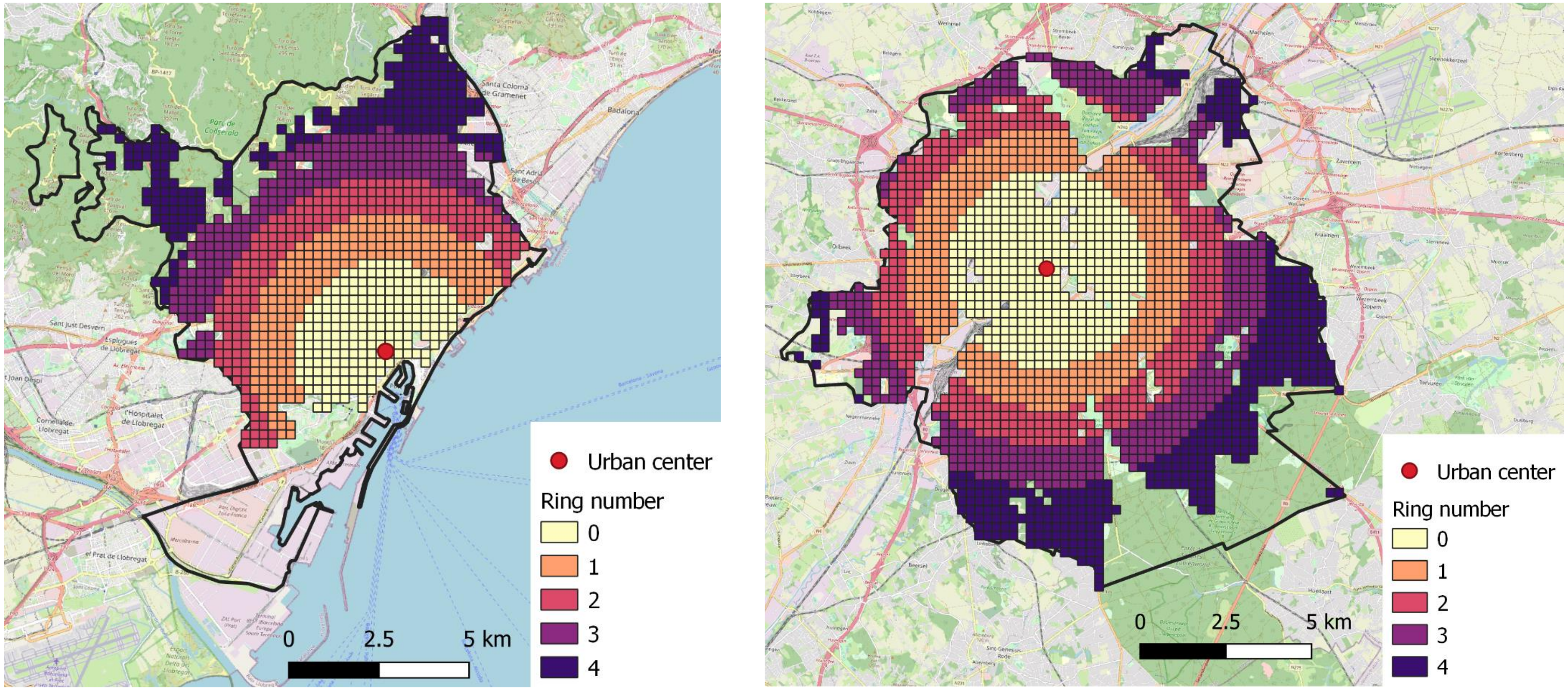

Figure S1. *An example of the division of the cities into rings is shown for Barcelona, Spain (left panel) and Brussel, Belgium (right panel).*

C) **Local Climate Zones (LCZs) classification.**

We retrieved the LCZ classification developed by Demuzere and colleagues (9,10) at 100m resolution for Europe. We overlaid the LCZ layer with our 250m grid cell layer and estimated the proportion of area corresponding to each LCZ for each of the grid cells. We excluded grid cells that had more than 80% of their area not covered by the LCZ layer (n = 1,208).

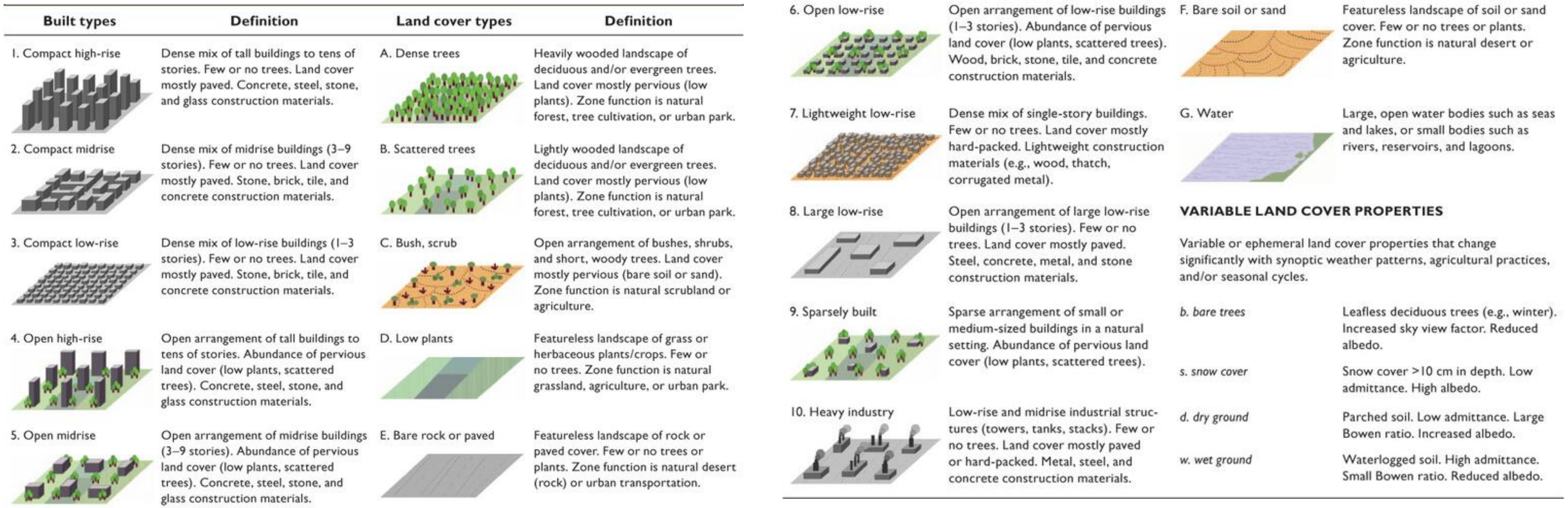

Built types	Definition	Land cover types	Definition
1. Compact high-rise	Dense mix of tall buildings to tens of stories. Few or no trees. Land cover mostly paved. Concrete, steel, stone, and glass construction materials.	A. Dense trees	Heavily wooded landscape of deciduous and/or evergreen trees. Land cover mostly pervious (low plants). Zone function is natural forest, tree cultivation, or urban park.
2. Compact midrise	Dense mix of midrise buildings (3–9 stories). Few or no trees. Land cover mostly paved. Stone, brick, tile, and concrete construction materials.	B. Scattered trees	Lightly wooded landscape of deciduous and/or evergreen trees. Land cover mostly pervious (low plants). Zone function is natural forest, tree cultivation, or urban park.
3. Compact low-rise	Dense mix of low-rise buildings (1–3 stories). Few or no trees. Land cover mostly paved. Stone, brick, tile, and concrete construction materials.	C. Bush, scrub	Open arrangement of bushes, shrubs, and short, woody trees. Land cover mostly pervious (bare soil or sand). Zone function is natural scrubland or agriculture.
4. Open high-rise	Open arrangement of tall buildings to tens of stories. Abundance of pervious land cover (low plants, scattered trees). Concrete, steel, stone, and glass construction materials.	D. Low plants	Featureless landscape of grass or herbaceous plants/crops. Few or no trees. Zone function is natural grassland, agriculture, or urban park.
5. Open midrise	Open arrangement of midrise buildings (3–9 stories). Abundance of pervious land cover (low plants, scattered trees). Concrete, steel, stone, and glass construction materials.	E. Bare rock or paved	Featureless landscape of rock or paved cover. Few or no trees or plants. Zone function is natural desert (rock) or urban transportation.
6. Open low-rise	Open arrangement of low-rise buildings (1–3 stories). Abundance of pervious land cover (low plants, scattered trees). Wood, brick, stone, tile, and concrete construction materials.	F. Bare soil or sand	Featureless landscape of soil or sand cover. Few or no trees or plants. Zone function is natural desert or agriculture.
7. Lightweight low-rise	Dense mix of single-story buildings. Few or no trees. Land cover mostly hard-packed. Lightweight construction materials (e.g., wood, thatch, corrugated metal).	G. Water	Large, open water bodies such as seas and lakes, or small bodies such as rivers, reservoirs, and lagoons.
8. Large low-rise	Open arrangement of large low-rise buildings (1–3 stories). Few or no trees. Land cover mostly paved. Steel, concrete, metal, and stone construction materials.	**VARIABLE LAND COVER PROPERTIES** Variable or ephemeral land cover properties that change significantly with synoptic weather patterns, agricultural practices, and/or seasonal cycles.	
9. Sparsely built	Sparse arrangement of small or medium-sized buildings in a natural setting. Abundance of pervious land cover (low plants, scattered trees).	*b. bare trees*	Leafless deciduous trees (e.g., winter). Increased sky view factor. Reduced albedo.
		s. snow cover	Snow cover >10 cm in depth. Low admittance. High albedo.
10. Heavy industry	Low-rise and midrise industrial structures (towers, tanks, stacks). Few or no trees. Land cover mostly paved or hard-packed. Metal, steel, and concrete construction materials.	*d. dry ground*	Parched soil. Low admittance. Large Bowen ratio. Increased albedo.
		w. wet ground	Waterlogged soil. High admittance. Small Bowen ratio. Reduced albedo.

Figure S2. *Description of Local Climate Zones (LCZs) categories from Stewart & Oke, 2012.*

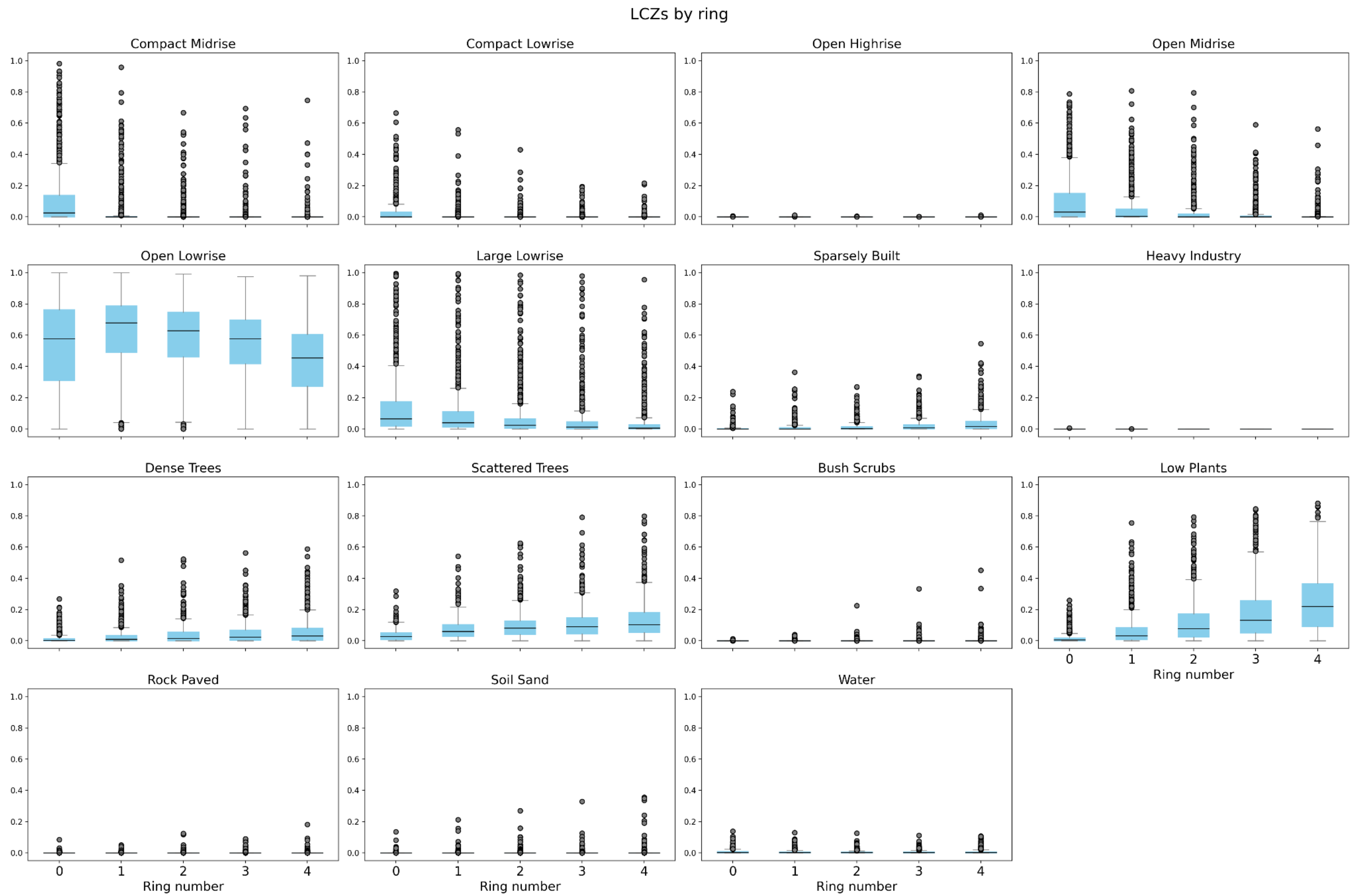

Figure S3. *Descriptive boxplots of LCZs data for all cities by ring. The proportion of each LCZ in each ring is shown. * Outliers are kept in the plots in order to show the complete distribution of the data that was employed in the UMAP analysis.*

Table S1. *Descriptive of LCZs data for all cities by ring.*

Variable	Ring	Mean	Median	IQR 25%	IQR 75%	Min	Max
Compact midrise (%)	0	11.7	2.6	0	13.9	0	98.2
	1	2.9	0	0	0.3	0	95.9
	2	1.3	0	0	0	0	66.8
	3	0.9	0	0	0	0	69.4
	4	0.5	0	0	0	0	74.7
Compact lowrise (%)	0	3.4	0.2	0	3.3	0	66.5
	1	0.9	0	0	0.1	0	55.7
	2	0.5	0	0	0	0	43.0
	3	0.3	0	0	0	0	19.4
	4	0.2	0	0	0	0	21.7
Open highrise (%)	0	0	0	0	0	0	0.6
	1	0	0	0	0	0	1.2
	2	0	0	0	0	0	0.5
	3	0	0	0	0	0	0.3
	4	0	0	0	0	0	1.2
Open midrise (%)	0	10.2	3.2	0	15.2	0	78.7
	1	5.5	0.4	0	5.2	0	80.8
	2	3.3	0	0	2.1	0	79.5
	3	1.9	0	0	0.7	0	59.1
	4	0.9	0	0	0.1	0	56.3
Open lowrise (%)	0	52.5	57.6	30.9	76.3	0	100
	1	61.7	68	48.9	78.8	0	100
	2	58.7	62.8	46.2	74.7	0	99.2

	3	54	57.6	41.8	69.9	0	97.5
	4	44.4	45.5	27.3	60.6	0	98.1
Large lowrise (%)	0	13.8	6.5	1.7	17.6	0	99.6
	1	9.8	3.9	1	11.2	0	99.3
	2	7.5	2.3	0.4	6.7	0	98.5
	3	5.7	1.2	0.1	4.7	0	97.9
	4	4	0.5	0	2.9	0	95.5
Sparsely built (%)	0	0.4	0	0	0.2	0	23.9
	1	1	0.1	0	0.9	0	36.4
	2	1.6	0.3	0	1.7	0	27.0
	3	2.3	0.7	0	2.8	0	33.7
	4	3.8	1.6	0.1	5.1	0	54.6
Heavy industry (%)	0	0	0	0	0	0	0.5
	1	0	0	0	0	0	0
	2	0	0	0	0	0	0
	3	0	0	0	0	0	0
	4	0	0	0	0	0	0
Dense trees (%)	0	1.4	0.3	0	1.5	0	26.9
	1	3	1	0	3.5	0	51.6
	2	4	1.6	0.1	5.8	0	52.3
	3	4.8	2.5	0.3	6.8	0	56.3
	4	6.1	3.2	0.4	8.2	0	58.8
Scattered trees (%)	0	3.7	2.7	0.8	5.3	0	32
	1	7.5	6.1	2.7	10.4	0	54.2
	2	9.7	8.2	4	12.9	0	62.5
	3	11	9	4.5	15	0	79.2

	4	13.3	10.3	5.4	18.2	0	79.9
Bush scrubs (%)	0	0	0	0	0	0	1.4
	1	0	0	0	0	0	4.1
	2	0.1	0	0	0	0	22.6
	3	0.2	0	0	0	0	33.3
	4	0.4	0	0	0	0	45.3
Low plants (%)	0	1.7	0.6	0	1.9	0	26
	1	6.7	3.3	0.8	8.5	0	75.5
	2	12.7	7.8	2.4	17.3	0	79.3
	3	17.9	13.1	5.1	26	0	84.5
	4	25.1	21.9	9	36.7	0	88.1
Rock paved (%)	0	0.1	0	0	0	0	8.5
	1	0.1	0	0	0	0	5.1
	2	0.1	0	0	0	0	12.4
	3	0.1	0	0	0	0	8.9
	4	0.2	0	0	0	0	18.1
Soil sand (%)	0	0.1	0	0	0	0	13.4
	1	0.2	0	0	0	0	21.1
	2	0.2	0	0	0	0	27.0
	3	0.2	0	0	0	0	32.8
	4	0.3	0	0	0	0	35.6
Water (%)	0	0.8	0.2	0	0.9	0	13.8
	1	0.6	0.2	0	0.7	0	13.0
	2	0.5	0.1	0	0.5	0	12.6
	3	0.5	0.1	0	0.6	0	11.1
	4	0.7	0.1	0	0.8	0	10.8

D) **Open Street Map (OSM) road classification.**

To evaluate the street design, we retrieved the density of distinct road typologies from the OSM database (11). We included road types as follows: motorized roads (formed by “motorway” and “trunk”), primary roads, secondary roads, tertiary roads, residential roads (formed by “unclassified”, “residential” and “living streets”), pedestrian zones and cycleways (**Table S2**). For each grid cell, we calculated the length in meters of each road type. Given inconsistencies in OSM data and overrepresentation of specific road types in some of the cities, we excluded from the analysis grids with values above the 99.5th percentile of each category to avoid outliers in the dataset.

Table S2. *Description of OSM road categories.*

Grouping category	Included OSM categories	Category definition
Motorized roads	Motorway	A restricted access major divided highway, normally with 2 or more running lanes plus emergency hard shoulder. Equivalent to the Freeway, Autobahn, etc..
	Motorway link	The link roads (slip roads/ramps) leading to/from a motorway from/to a motorway or lower-class highway. Normally with the same motorway restrictions.
	Trunk	The most important roads in a country's system that aren't motorways (not necessarily a divided highway).
	Trunk link	The link roads (slip roads/ramps) leading to/from a trunk road from/to a trunk road or lower-class highway.
Primary roads	Primary	The next most important roads in a country's system (often link larger towns).
	Primary link	The link roads (slip roads/ramps) leading to/from a primary road from/to a primary road or lower-class highway.
Secondary roads	Secondary	The next most important roads in a country's system (often link towns).
	Secondary link	The link roads (slip roads/ramps) leading to/from a secondary road from/to a secondary road or lower-class highway.
Tertiary roads	Tertiary	The next most important roads in a country's system (often link smaller towns and villages).
	Tertiary link	The link roads (slip roads/ramps) leading to/from a tertiary road from/to a tertiary road or lower-class highway.
Residential roads	Unclassified	The least important through-roads in a country's system, i.e. minor roads of a lower classification than tertiary, but which serve a purpose other than access to properties (often link villages and hamlets).
	Residential	Roads which serve as an access to housing, without the function of connecting settlements. Often lined with housing.
	Living streets	Residential streets where pedestrians have legal priority over cars, speeds are kept very low and where children are allowed to play on the street.
Pedestrian	Pedestrian	Roads used mainly/exclusively for pedestrians in shopping and some residential areas which may allow access by motorized vehicles only for very limited periods of the day.
Cycleways	Cycleway	Path for designated cycleways.

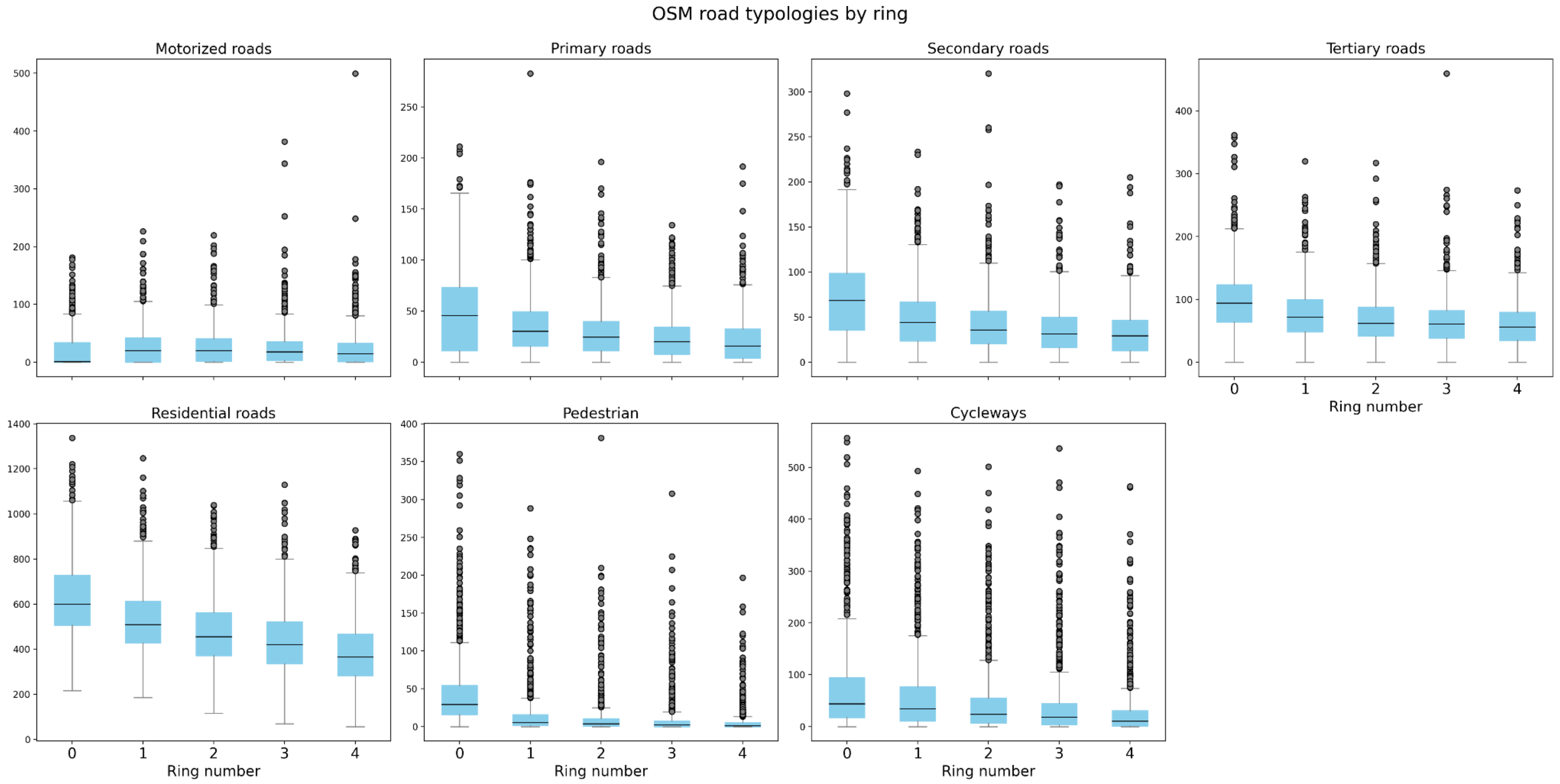

Figure S4. *Descriptive boxplots of OSM road typologies for all cities by ring. The mean length per grid cell in meters for each ring is shown. * Outliers are kept in the plots in order to show the complete distribution of the data that was employed in the UMAP analysis.*

Table S3. *Descriptive of OSM road typologies for all cities by ring.*

Variable	Ring	Mean	Median	IQR 25%	IQR 75%	Min	Max
Motorized roads (mean meters/grid cell)	0	21	1	0	34	0	181
	1	27	20	0	42	0	226
	2	28	20	2	41	0	220
	3	25	18	3	36	0	381
	4	24	15	1	33	0	499
Primary roads (mean meters/grid cell)	0	48	46	11	74	0	211
	1	35	30	16	50	0	283
	2	29	25	11	40	0	196
	3	25	20	8	35	0	134
	4	22	16	4	33	0	192
Secondary roads (mean meters/grid cell)	0	70	68	35	99	0	298
	1	49	44	24	67	0	233
	2	42	36	21	57	0	320
	3	36	32	16	50	0	197
	4	33	29	13	47	0	205
Tertiary roads (mean meters/grid cell)	0	98	94	64	123	0	361
	1	77	72	48	100	0	319
	2	68	62	42	88	0	317
	3	64	61	39	82	0	459
	4	59	56	35	79	0	273
Residential roads (mean meters/grid cell)	0	630	599	507	729	216	1337
	1	531	510	429	612	185	1248
	2	476	455	371	563	116	1039
	3	439	421	335	522	70	1130

	4	386	366	283	467	57	928
Pedestrian (mean meters/grid cell)	0	45	29	16	54	0	360
	1	17	6	2	16	0	288
	2	12	4	1	11	0	381
	3	9	2	0	8	0	308
	4	7	1	0	5	0	197
Cycleways (mean meters/grid cell)	0	74	44	17	94	0	557
	1	60	35	11	77	0	493
	2	49	24	7	56	0	501
	3	41	18	3	45	0	537
	4	30	11	1	31	0	464

E) **Motorized traffic flows.**

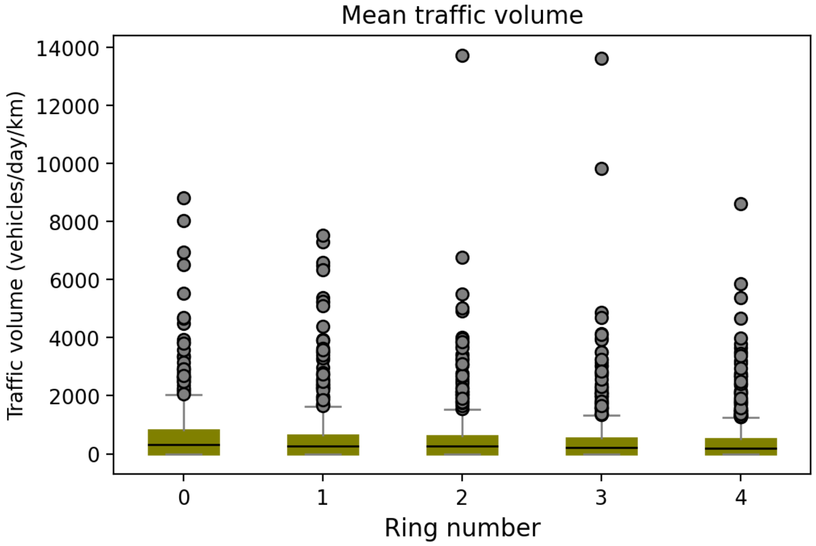

Figure S5. *Descriptive boxplot of traffic volume for all cities by ring.*

Table S4. *Descriptive of traffic volume for all cities by ring.*

Variable	Ring	Mean	Median	IQR 25%	IQR 75%	Min	Max
Traffic volume (vehicles/day/km)	0	584	310	0	827	0	8,805
	1	519	277	0	656	0	7,525
	2	482	266	0	617	0	13,727
	3	433	218	0	537	0	13,613
	4	400	183	0	508	0	8,617

F) **Surface Urban Heat Island (SUHI).**

We estimated the SUHI as the difference between the mean summer rural Land Surface Temperature (LST) and the median summer LST recorded in each urban grid cell. Data was retrieved from Landsat-8 images for 2015 (12) at 30 × 30m resolution, with data acquisition time varying between 9 and 11 am for Europe. We implemented a cleanup process for clouds and other potential quality issues. Specifically, we employed the 'QA_PIXEL' band: Pixel quality attributes generated from the CFMASK algorithm. This allows us to filter out pixels affected by clouds, snow, or shadows (cirrus, snow, and shadows) in all images, irrespective of whether they are in urban or rural areas. To define the surrounding rural area, we took a buffer zone of 6 kilometers surrounding each city, to ensure sufficient coverage, and defined the rural area based on Corine Land Cover agricultural, forest and natural areas categories (13). Specifically, the categories included were: non-irrigated arable land, permanently irrigated land, rice fields, vineyards, fruit trees and berry plantations, olive groves, pastures, annual crops associated with permanent crops, complex cultivation patterns, land principally occupied by agriculture with significant areas of natural vegetation, agroforestry areas, broad-leaved forest, coniferous forest, mixed forest, natural grasslands, moors and heartland, sclerophyllous vegetation and transitional woodland-shrub. We filtered out blue spaces to avoid underestimating the average rural LST (14) and excluded the CLC green urban areas category to prevent the inclusion of urban parks from neighboring cities in the measurement of surrounding greenness.

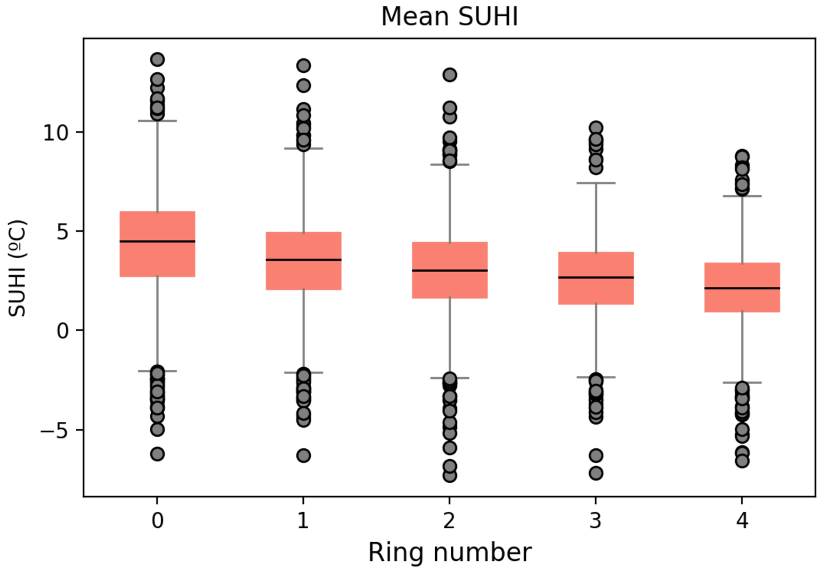

Figure S6. *Descriptive boxplot of SUHI for all cities by ring.*

Table S5. *Descriptive of SUHI for all cities by ring.*

Variable	Ring	Mean (SD)	Median	IQR 25%	IQR 75%	Min	Max
SUHI (ºC)	0	4.2 (3)	4.5	2.8	6	-6.2	13.7
	1	3.4 (2.6)	3.6	2.1	4.9	-6.3	13.4
	2	3 (2.4)	3	1.7	4.4	-7.3	12.9
	3	2.6 (2.2)	2.7	1.4	3.9	-7.2	10.2
	4	2.1 (2.1)	2.2	1	3.4	-6.6	8.8

G) **Tropospheric Nitrogen Dioxide (NO_2).**

Tropospheric NO_2 is a short-lived tracer to map the footprint of predominantly anthropogenic emissions from combustion processes. Natural contributions are confined to lightning (15) and microbial processes in soils (16). Therefore, it has proven to be a suitable tracer to delineate urban pollution islands and pollution hot spots (17–20). In this study, data from TROPOMI, the sensor aboard the Sentinel-5 Precursor satellite as part of the Copernicus Space Infrastructure, was used to obtain observations of tropospheric NO_2 (21). Specifically, the Level 2 tropospheric NO_2 data product (Version 1.2) using the algorithm developed by van Geffen et al., (2020) and provided by the European Space Agency (ESA) was exploited (22). The nominal spatial resolution of the observations (pixels) was 3.5 x 7.5 km^2 and was improved to 3.5 x 5.5 km^2 on August 6, 2019. The tropospheric NO_2 vertical column densities were retrieved with a conservative quality flag greater than 75. In a next step, all Level 2 products over Europe from 1st January 2019 to 31st December 2019 were oversampled onto a regular grid of 0.0025° x 0.0025° spatial resolution, which corresponds to ~100 to 200m depending on the latitude, following Müller et al., (2022) (18). By means of the temporal aggregation and the rigorous tiling approach of the pixels, the spatial resolution could be increased for persistent emission sources and anthropogenic NO_2 footprints. The resulting yearly mean can be considered a robust estimate to delineate the NO_2 footprints of the European cities. The year 2019 was chosen as the most recent year not influenced by any COVID-19 measures or effects. The data has proven to be feasible to analyze the shape of urban pollution islands of megacities (19), smaller cities with complex terrain (20) and emission hot spots for the contiguous United States (23) and Germany (18). Due to the physical limitations of the measurements, intra-urban hot spots cannot fully be resolved. Thus, we consider the data to represent urban background conditions. However, the observational data is not influenced by any chemical-transport modeling, assumptions on emissions, machine learning or geostatistical modelling.

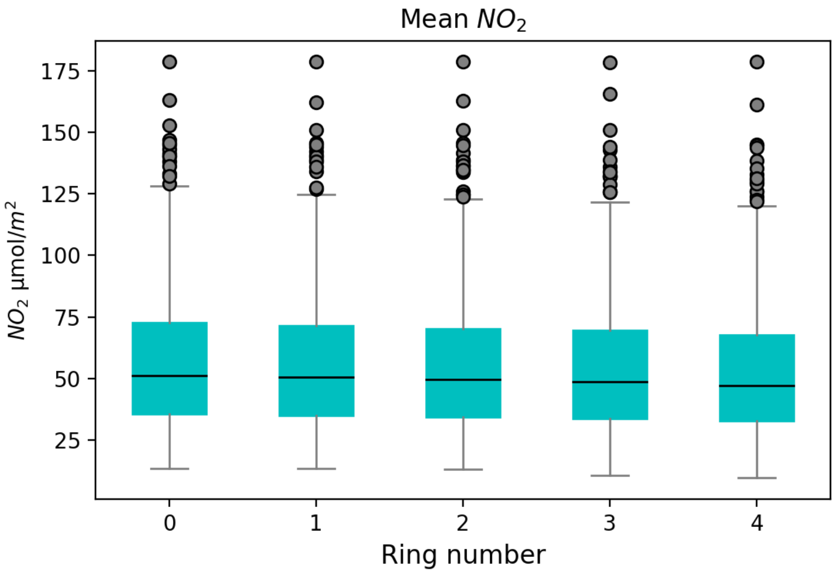

Figure S7. *Descriptive boxplot of tropospheric NO_2 for all cities by ring.*

Table S6. *Descriptive of tropospheric NO_2 for all cities by ring.*

Variable	Ring	Mean	Median	IQR 25%	IQR 75%	Min	Max
Tropospheric NO_2 (μmol/m^2)	0	56.7	51.3	35.5	72.6	13.6	178.5
	1	56.1	50.6	35.0	71.5	13.7	178.6
	2	55.4	49.6	34.4	70.1	13.1	178.6
	3	54.5	48.9	33.9	69.4	10.6	178.2
	4	53.1	47.2	32.7	67.8	9.6	178.7

H) **CO_2 emissions.**

We retrieved CO_2 emissions data from the Open-source Data Inventory for Anthropogenic CO_2 (ODIAC) (24), which provides CO_2 emissions from fossil-fuel combustion at 1 x 1 km resolution for 2019. In this dataset, national emissions are spatialized based on satellite night-time light data and power plant location and profiles (24). To estimate the per capita emissions, we overlaid the CO_2 emissions layer with the 250m grid cell layer and distributed the CO_2 emissions proportionally based on the intersecting area of the 250m grid cells with the 1 km grid cells. For each 250m grid cell we calculated the CO_2 emissions as follows: Grid cell emissions (250m) = Intersection area * Total CO_2 emissions (1 km) / Total area CO_2 grid (1 km). Afterwards, to consider that each 250m grid cell might intersect with more than one 1 km CO_2 grid, we did an aggregate sum by the 250m grid cells to obtain the total CO_2 emissions at 250m resolution. We divided the emissions between the population in each 250m grid cell to obtain the CO_2 per capita emissions in metric tons.

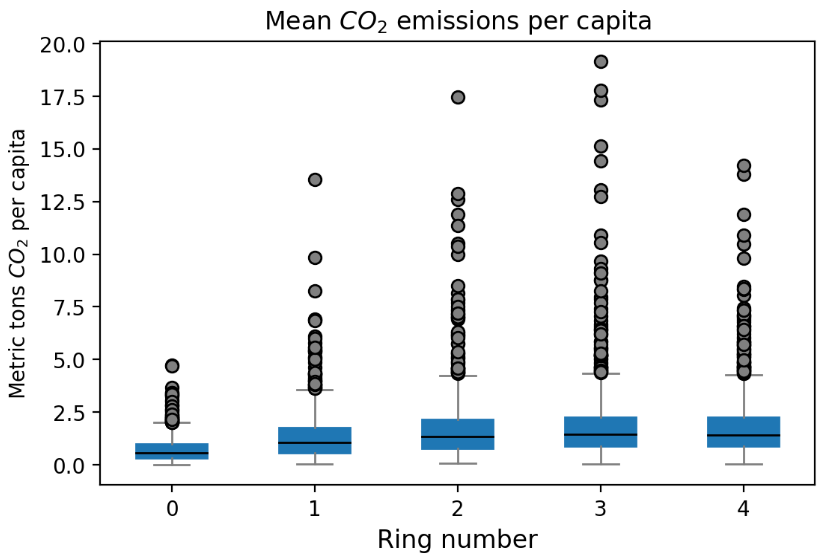

Figure S8. *Descriptive boxplot of CO_2 per capita emissions for all cities by ring.*

Table S7. *Descriptive of CO_2 per capita emissions for all cities by ring.*

Variable	Ring	Mean	Median	IQR 25%	IQR 75%	Min	Max
CO_2 per capita emissions (metric tons)	0	0.8	0.6	0.3	1	0	4.7
	1	1.4	1.1	0.6	1.8	0	13.5
	2	1.7	1.3	0.8	2.2	0.1	17.5
	3	1.9	1.4	0.9	2.3	0.1	19.2
	4	1.9	1.4	0.9	2.3	0	14.2

I) **Main analysis.**

To identify and characterize distinct urban configuration types, we applied the Uniform Manifold Approximation and Projection for Dimension Reduction (UMAP), followed by the k-means clustering algorithm. UMAP is a novel non-linear dimension reduction algorithm able to learn the manifold structure of large input datasets and produce a low-dimensional embedding that preserves the basic topological structure of the manifold (25). UMAP was chosen for this analysis because it outperforms previous dimension reduction algorithms, such as t-SNE, in terms of speed and better preservation of the data's global structure, which potentially results in more meaningful inter-cluster relations (25).

i) Variables correlation.

We used LCZs and OSM variables from each of the five rings for each city as input data for the UMAP algorithm. For establishing the relative strength of the correlations in our dataset and in order to prevent a distorted embedding, we evaluated the distribution of correlations (**Figure S9**). We defined as outliers correlation values greater than r = 0.55 (**Figure S10**) and established it as exclusion criteria for conducting UMAP. Accordingly, we excluded the pedestrian and residential roads categories from OSM as both variables presented correlations equal to or above r = 0.55 with the Compact Midrise and Low Plants variables, respectively. In addition, we excluded LCZs categories with null values at percentile 75% (i.e. open highrise, compact lowrise, heavy industry, bush scrubs, rock paved and soil sand) to avoid distortions of the embedding (25,26) (**Figure S3, Table S1**).

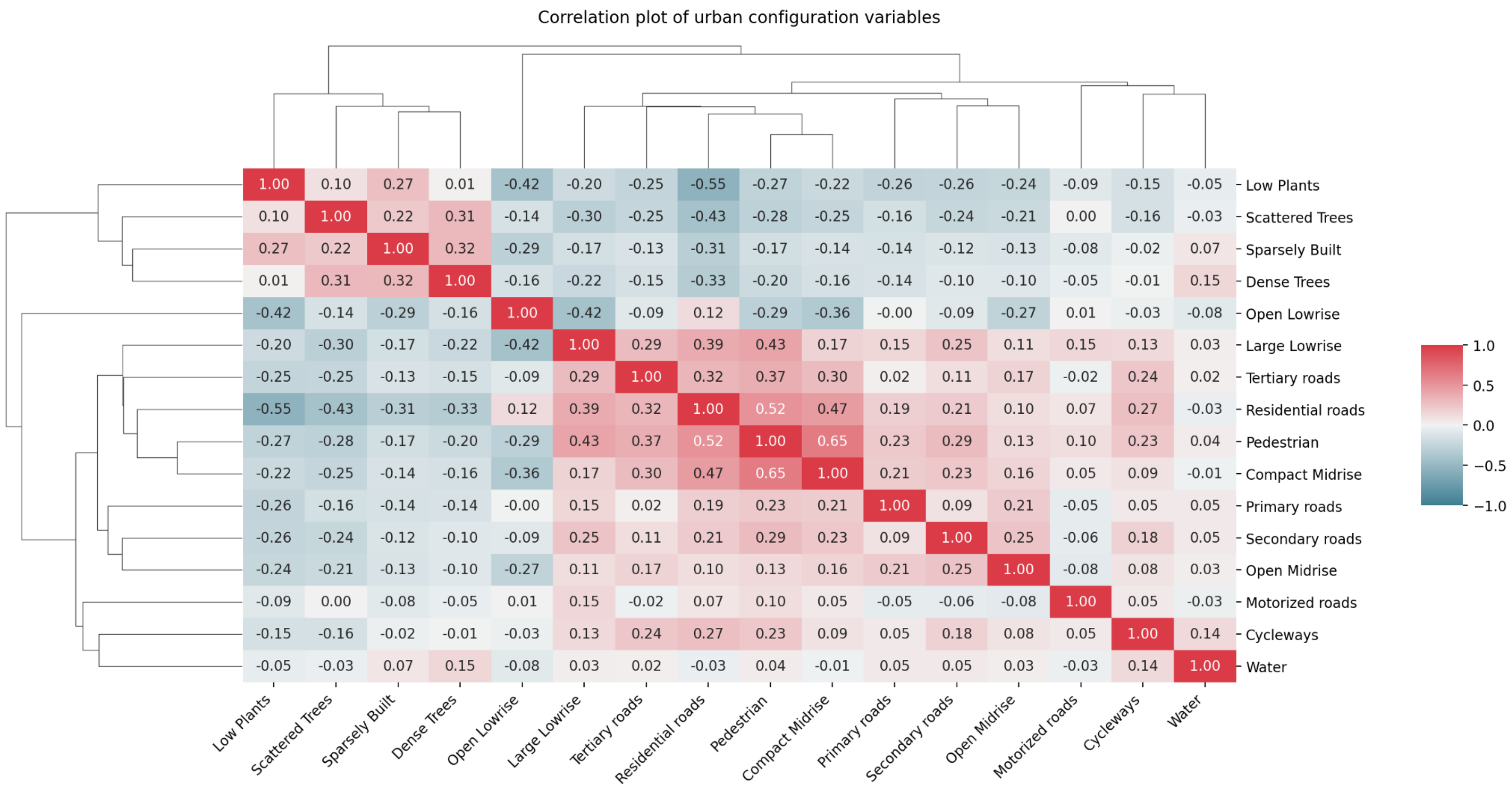

Figure S9. *Correlation plot of urban configuration variables considered for the analysis.*

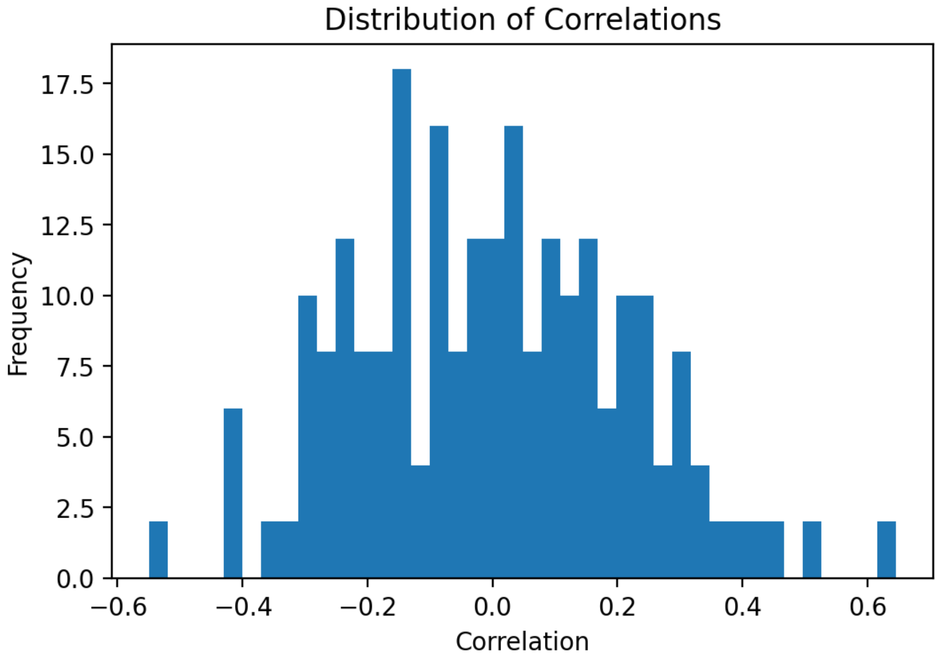

Figure S10. Distribution of correlations in our dataset.

ii) UMAP and k-means parameter optimization.

The choice of UMAP parameters (i.e. *n_neighbors and min_dist*) is crucial and allows to balance between the local and global structure of the data in the final projection (27). A lower value of *n_neighbors* pushes the UMAP algorithm to focus more on the local structure, while *min_dist* controls how tightly points are clustered together, with lower values resulting in higher clustering (27). For this study, we opted for *n_neighbors* = 15 and *min_dist* = 0 as UMAP parameters. These choices emphasize local data relationships while maintaining a connection with the broader structure. The choice of the *n_neighbors* parameter was further validated using the trustworthiness score for values between 0 and 30 (28) (**Figure S11**). To select the optimal number of clusters for the k-means algorithm, we applied the Elbow method and set the number at k = 4 (**Figure S11**).

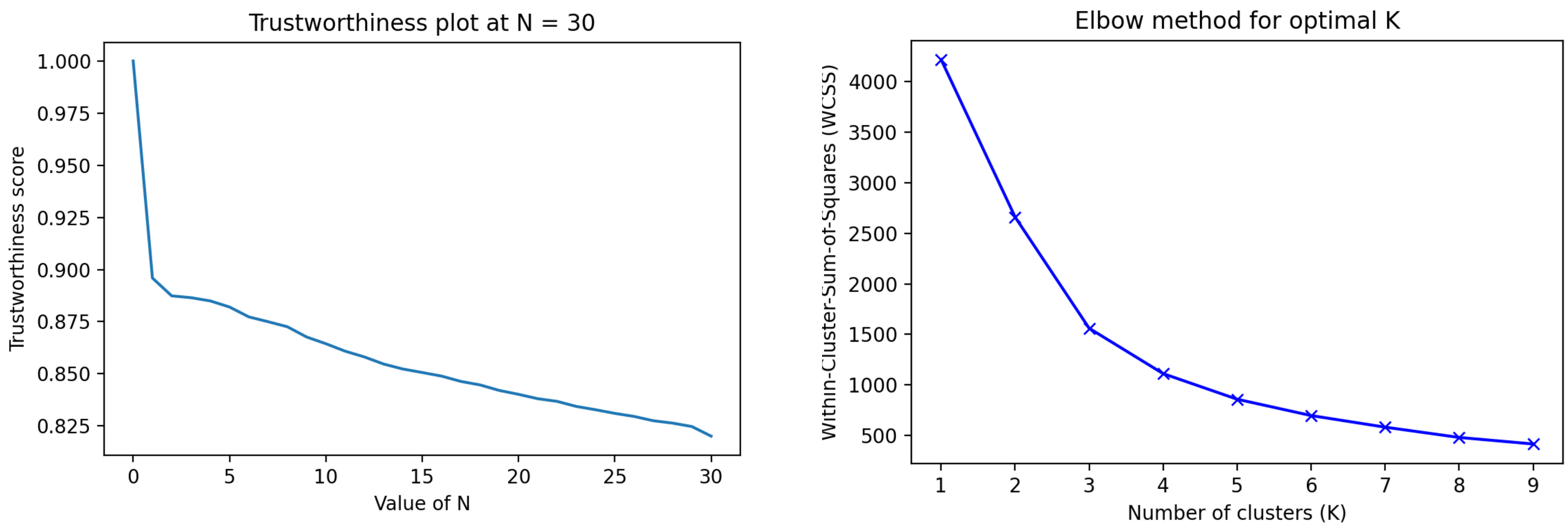

Figure S11. *Trustworthiness score plot to validate the choice of the n_neighbors parameter for the UMAP algorithm (left panel) and Elbow method plot to identify the optimal number of clusters for the k-means clustering algorithm (right panel). * A trustworthiness score above 0.8 represents a good preservation of the local data structure in the low-dimensional space.*

iii) Results.

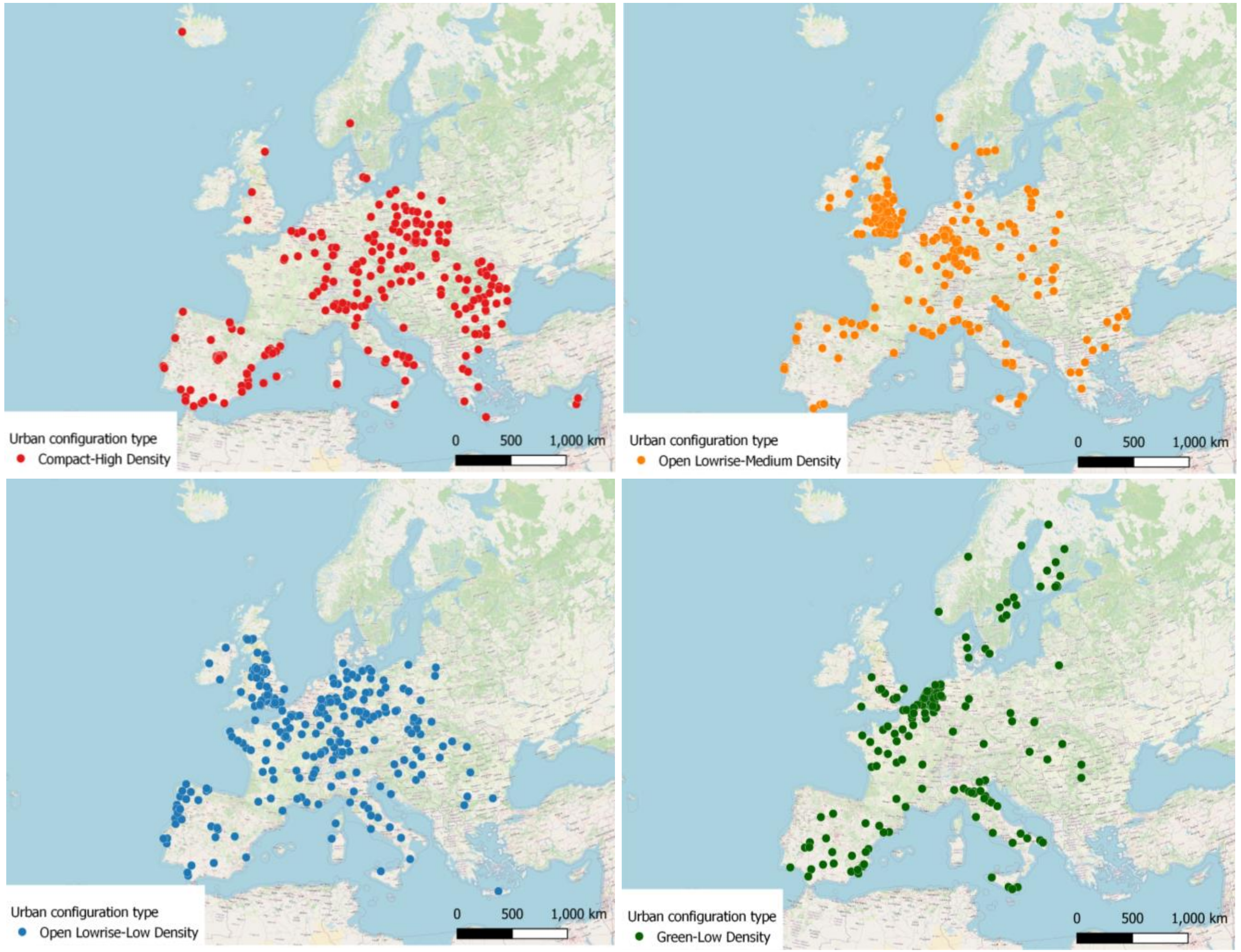

Figure S12. Geographic location of each urban configuration type. The geographic location of all urban configuration types was generally widespread, with Compact-High Density cities prevailing in Southern and Eastern Europe, Open Lowrise-Medium Density and Open Lowrise-Low Density in Western Europe and the UK and Green-Low Density cities in Northern Europe and the Netherlands.

Table S8. Dunn's test results for motorized traffic flows and the SUHI intensity.

	Dunn's test (traffic flows)			Dunn's test (SUHI intensity)		
Ring	**Compared urban configuration types**		**p-value**	**Compared urban configuration types**		**p-value**
0	Compact-High Density	Open Lowrise-Medium Density	0.007 **	Compact-High Density	Open Lowrise-Medium Density	< 0.001 ***
	Compact-High Density	Open Lowrise-Low Density	< 0.001 ***	Compact-High Density	Open Lowrise-Low Density	< 0.001 ***
	Compact-High Density	Green-Low Density	< 0.001 ***	Compact-High Density	Green-Low Density	0.33
	Open Lowrise-Medium Density	Open Lowrise-Low Density	< 0.001 ***	Open Lowrise-Medium Density	Open Lowrise-Low Density	0.96
	Open Lowrise-Medium Density	Green-Low Density	0.03 *	Open Lowrise-Medium Density	Green-Low Density	< 0.001 ***
	Open Lowrise-Low Density	Green-Low Density	0.27	Open Lowrise-Low Density	Green-Low Density	< 0.001 ***
1	Compact-High Density	Open Lowrise-Medium Density	0.002 **	Compact-High Density	Open Lowrise-Medium Density	0.003 **
	Compact-High Density	Open Lowrise-Low Density	< 0.001 ***	Compact-High Density	Open Lowrise-Low Density	0.13
	Compact-High Density	Green-Low Density	< 0.001 ***	Compact-High Density	Green-Low Density	0.03 *
	Open Lowrise-Medium Density	Open Lowrise-Low Density	< 0.001 ***	Open Lowrise-Medium Density	Open Lowrise-Low Density	0.13
	Open Lowrise-Medium Density	Green-Low Density	0.03 *	Open Lowrise-Medium Density	Green-Low Density	< 0.001 ***
	Open Lowrise-Low Density	Green-Low Density	0.25	Open Lowrise-Low Density	Green-Low Density	< 0.001 ***
2	Compact-High Density	Open Lowrise-Medium Density	< 0.001 ***	Compact-High Density	Open Lowrise-Medium Density	< 0.001 ***
	Compact-High Density	Open Lowrise-Low Density	< 0.001 ***	Compact-High Density	Open Lowrise-Low Density	0.35

	Compact-High Density	Green-Low Density	< 0.001 ***	Compact-High Density	Green-Low Density	0.002 **
	Open Lowrise-Medium Density	Open Lowrise-Low Density	< 0.001 ***	Open Lowrise-Medium Density	Open Lowrise-Low Density	0.01 *
	Open Lowrise-Medium Density	Green-Low Density	0.08	Open Lowrise-Medium Density	Green-Low Density	< 0.001 ***
	Open Lowrise-Low Density	Green-Low Density	0.08	Open Lowrise-Low Density	Green-Low Density	< 0.001 ***
3	Compact-High Density	Open Lowrise-Medium Density	< 0.001 ***	Compact-High Density	Open Lowrise-Medium Density	< 0.001 ***
	Compact-High Density	Open Lowrise-Low Density	< 0.001 ***	Compact-High Density	Open Lowrise-Low Density	0.35
	Compact-High Density	Green-Low Density	< 0.001 ***	Compact-High Density	Green-Low Density	0.005 **
	Open Lowrise-Medium Density	Open Lowrise-Low Density	< 0.001 ***	Open Lowrise-Medium Density	Open Lowrise-Low Density	< 0.001 ***
	Open Lowrise-Medium Density	Green-Low Density	0.01 *	Open Lowrise-Medium Density	Green-Low Density	< 0.001 ***
	Open Lowrise-Low Density	Green-Low Density	0.44	Open Lowrise-Low Density	Green-Low Density	< 0.001 ***
4	Compact-High Density	Open Lowrise-Medium Density	0.003 **	Compact-High Density	Open Lowrise-Medium Density	< 0.001 ***
	Compact-High Density	Open Lowrise-Low Density	< 0.001 ***	Compact-High Density	Open Lowrise-Low Density	0.04 *
	Compact-High Density	Green-Low Density	< 0.001 ***	Compact-High Density	Green-Low Density	0.11
	Open Lowrise-Medium Density	Open Lowrise-Low Density	< 0.001 ***	Open Lowrise-Medium Density	Open Lowrise-Low Density	< 0.001 ***
	Open Lowrise-Medium Density	Green-Low Density	0.02 *	Open Lowrise-Medium Density	Green-Low Density	< 0.001 ***
	Open Lowrise-Low Density	Green-Low Density	0.25	Open Lowrise-Low Density	Green-Low Density	< 0.001 ***

Table S9. Dunn's test results for the NO_2 exposure and CO_2 per capita emissions.

	Dunn's test (NO_2 exposure)			Dunn's test (CO_2 emissions)		
Ring	**Compared urban configuration types**		**p-value**	**Compared urban configuration types**		**p-value**
0	Compact-High Density	Open Lowrise-Medium Density	0.22	Compact-High Density	Open Lowrise-Medium Density	< 0.001 ***
	Compact-High Density	Open Lowrise-Low Density	0.007 **	Compact-High Density	Open Lowrise-Low Density	< 0.001 ***
	Compact-High Density	Green-Low Density	0.03 *	Compact-High Density	Green-Low Density	< 0.001 ***
	Open Lowrise-Medium Density	Open Lowrise-Low Density	< 0.001 ***	Open Lowrise-Medium Density	Open Lowrise-Low Density	0.10
	Open Lowrise-Medium Density	Green-Low Density	0.001 **	Open Lowrise-Medium Density	Green-Low Density	0.36
	Open Lowrise-Low Density	Green-Low Density	0.79	Open Lowrise-Low Density	Green-Low Density	0.59
1	Compact-High Density	Open Lowrise-Medium Density	0.23	Compact-High Density	Open Lowrise-Medium Density	< 0.001 ***
	Compact-High Density	Open Lowrise-Low Density	0.007 **	Compact-High Density	Open Lowrise-Low Density	< 0.001 ***
	Compact-High Density	Green-Low Density	0.03 *	Compact-High Density	Green-Low Density	< 0.001 ***
	Open Lowrise-Medium Density	Open Lowrise-Low Density	< 0.001 ***	Open Lowrise-Medium Density	Open Lowrise-Low Density	< 0.001 ***
	Open Lowrise-Medium Density	Green-Low Density	0.001 **	Open Lowrise-Medium Density	Green-Low Density	< 0.001 ***
	Open Lowrise-Low Density	Green-Low Density	0.81	Open Lowrise-Low Density	Green-Low Density	0.21
2	Compact-High Density	Open Lowrise-Medium Density	0.24	Compact-High Density	Open Lowrise-Medium Density	< 0.001 ***
	Compact-High Density	Open Lowrise-Low Density	0.006 **	Compact-High Density	Open Lowrise-Low Density	< 0.001 ***

	Compact-High Density	Green-Low Density	0.03 *	Compact-High Density	Green-Low Density	< 0.001 ***
	Open Lowrise-Medium Density	Open Lowrise-Low Density	< 0.001 ***	Open Lowrise-Medium Density	Open Lowrise-Low Density	< 0.001 ***
	Open Lowrise-Medium Density	Green-Low Density	< 0.001 ***	Open Lowrise-Medium Density	Green-Low Density	< 0.001 ***
	Open Lowrise-Low Density	Green-Low Density	0.83	Open Lowrise-Low Density	Green-Low Density	0.08
3	Compact-High Density	Open Lowrise-Medium Density	0.25	Compact-High Density	Open Lowrise-Medium Density	0.02 **
	Compact-High Density	Open Lowrise-Low Density	0.008 **	Compact-High Density	Open Lowrise-Low Density	< 0.001 ***
	Compact-High Density	Green-Low Density	0.02 *	Compact-High Density	Green-Low Density	< 0.001 ***
	Open Lowrise-Medium Density	Open Lowrise-Low Density	< 0.001 ***	Open Lowrise-Medium Density	Open Lowrise-Low Density	< 0.001 ***
	Open Lowrise-Medium Density	Green-Low Density	< 0.001 ***	Open Lowrise-Medium Density	Green-Low Density	0.002 **
	Open Lowrise-Low Density	Green-Low Density	0.92	Open Lowrise-Low Density	Green-Low Density	0.91
4	Compact-High Density	Open Lowrise-Medium Density	0.17	Compact-High Density	Open Lowrise-Medium Density	0.46
	Compact-High Density	Open Lowrise-Low Density	0.01 *	Compact-High Density	Open Lowrise-Low Density	0.28
	Compact-High Density	Green-Low Density	0.04 *	Compact-High Density	Green-Low Density	0.22
	Open Lowrise-Medium Density	Open Lowrise-Low Density	< 0.001 ***	Open Lowrise-Medium Density	Open Lowrise-Low Density	0.73
	Open Lowrise-Medium Density	Green-Low Density	< 0.001 ***	Open Lowrise-Medium Density	Green-Low Density	0.56
	Open Lowrise-Low Density	Green-Low Density	0.90	Open Lowrise-Low Density	Green-Low Density	0.78

J) **Validation of the NO_2 exposure and CO_2 emissions variables.**

i) CO_2 per capita emission from CAMS.

To verify the CO_2 metric, we additionally explored the CO_2 emissions reported in the state-of-the-art Copernicus Atmosphere Monitoring Service (CAMS) regional inventory (version 7) for the residential and transport sectors (29). These sectors were chosen to better align with the ODIAC dataset. Since the CO_2 per capita emissions were extracted for residential grid cells, excluding industrial and port areas and their associated emissions, it was considered that focusing on residential and transport emissions would more accurately reflect the emission sources captured by ODIAC in our dataset. CAMS emissions were available at 0.1 x 0.05º resolution for the years 2000-2021 (30). We overlaid these emissions with our city boundaries and extracted the total emissions for each city. Per capita emissions were then calculated by dividing the total emissions by the total city population.

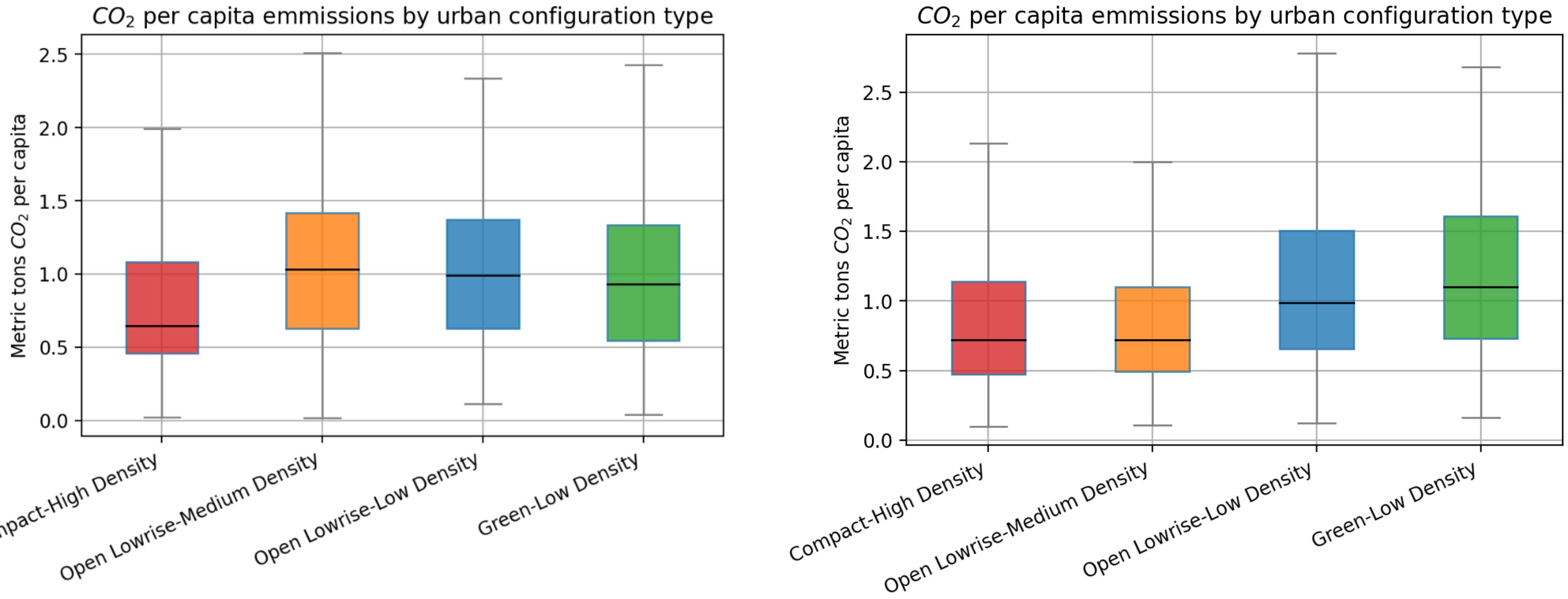

Figure S13. *CO_2 per capita emissions from the CAMS database for the residential sector (left panel) and the transport sector (right panel) by urban configuration type.*

Table S10. *CO_2 per capita emissions from CAMS by urban configuration types.*

	Compact-High Density			Open Lowrise-Medium Density			Open Lowrise-Low Density			Green-Low Density		
	Mean (SE)	**95% CI**		**Mean (SE)**	**95% CI**		**Mean (SE)**	**95% CI**		**Mean (SE)**	**95% CI**	
CO_2 per capita emissions – residential sector (metric tons)	0.9 (0.1)	0.8	1.1	1.2 (0.1)	1.1	1.3	1.2 (0.1)	1	1.3	1 (0.1)	0.9	1.1
CO_2 per capita emissions – transport sector (metric tons)	1 (0.1)	0.9	1.1	0.9 (0.1)	0.8	1	1.3 (0.1)	1.1	1.4	1.3 (0.1)	1.1	1.4

Table S11. *Dunn´s test results for CO_2 per capita emission from CAMS database (residential sector).*

Dunn's test		
Compared urban configuration types		**p-value**
Compact-High Density	Open Lowrise-Medium Density	<0.001***
Compact-High Density	Open Lowrise-Low Density	<0.001***
Compact-High Density	Green-Low Density	0.002 **
Open Lowrise-Medium Density	Open Lowrise-Low Density	0.71
Open Lowrise-Medium Density	Green-Low Density	0.10
Open Lowrise-Low Density	Green-Low Density	0.18

Table S12. *Dunn´s test result for CO_2 per capita emissions from CAMS database (transport sector).*

Dunn's test		
Compared urban configuration types		**p-value**
Compact-High Density	Open Lowrise-Medium Density	0.80
Compact-High Density	Open Lowrise-Low Density	<0.001***
Compact-High Density	Green-Low Density	<0.001***
Open Lowrise-Medium Density	Open Lowrise-Low Density	<0.001***
Open Lowrise-Medium Density	Green-Low Density	<0.001***
Open Lowrise-Low Density	Green-Low Density	0.18

ii) NO_2 exposure.

To validate the NO_2 proxy, we employed NO_2 measurements from official monitoring stations, available through the European Air Quality e-Reporting system (31). We extracted annual mean values for 2019 from background stations located in urban and suburban areas, considering only stations with ≥ 75% data coverage. We overlaid the station coordinates with our city boundaries to identify the stations within each city and then calculated the mean NO_2 levels from all stations for each city. Data was available for 516 cities.

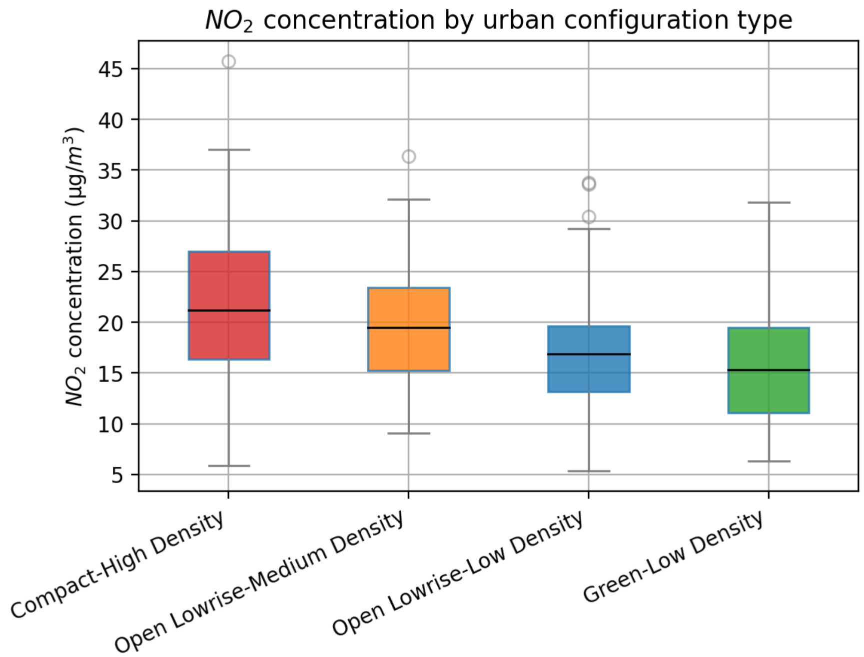

Figure S14. *Mean NO_2 concentration by urban configuration type.*

Table S13. *NO_2 concentration by urban configuration type.*

	Compact-High Density			Open Lowrise-Medium Density			Open Lowrise-Low Density			Green-Low Density		
NO_2 concentration ($\mu g/m^3$)	**Mean (SE)**	**95% CI**		**Mean (SE)**	**95% CI**		**Mean (SE)**	**95% CI**		**Mean (SE)**	**95% CI**	
	21.5 (0.6)	20.3	22.6	19.4 (0.4)	18.5	20.3	17.1 (0.5)	16.1	18	15.8 (0.6)	14.5	17

Table S14. *Dunn´s test results for NO_2 concentration.*

Dunn's test		
Compared urban configuration types		**p-value**
Compact-High Density	Open Lowrise-Medium Density	0.04 *
Compact-High Density	Open Lowrise-Low Density	< 0.001 ***
Compact-High Density	Green-Low Density	< 0.001 ***
Open Lowrise-Medium Density	Open Lowrise-Low Density	< 0.001 ***
Open Lowrise-Medium Density	Green-Low Density	< 0.001 ***
Open Lowrise-Low Density	Green-Low Density	0.17

K) **Sensitivity analyses.**

i) Exclusion of Mediterranean cities.

Table S15. *List of Mediterranean cities.*

Country	City name	Country	City name	Country	City name	Country	City name	Country	City name
Cyprus	Lefkosia	Spain	Rubi	Spain	Torrejon de Ardoz	Italy	Campobasso	Portugal	Almada
Cyprus	Lemesos	Spain	Ciudad Real	Spain	Alcobendas	Italy	Caserta	Portugal	Odivelas
Greece	Athina	Spain	Benidorm	Spain	Alcala de Guadaira	Italy	Taranto	Portugal	Viseu
Greece	Thessaloniki	Spain	Viladecans	Spain	Alcoy	Italy	Potenza	Portugal	Barreiro
Greece	Petra	Spain	Ponferrada	Spain	Avila	Italy	Catanzaro	Portugal	Sintra
Greece	Irakleio	Spain	San Sebastian de los Reyes	Spain	Benalmadena	Italy	Reggio di Calabria	Portugal	Vila Franca de Xira
Greece	Larisa	Spain	Zamora	Spain	Chiclana de la Frontera	Italy	Sassari		
Greece	Volos	Spain	Fuengirola	Spain	Collado Villalba	Italy	Cagliari		
Greece	Ioannina	Spain	Cerdanyola del Valles	Spain	Cuenca	Italy	Foggia		
Greece	Kavala	Spain	Sanlucar de Barrameda	Spain	Eivissa	Italy	Salerno		
Greece	Kalamata	Spain	Vilanova i la Geltru	Spain	Linares	Italy	La Spezia		
Greece	Chania	Spain	Prat de Llobregat, El	Spain	Lorca	Italy	Lecce		
Greece	Xanthi	Spain	Linea de la Concepcion, La	Spain	Merida	Italy	Barletta		
Greece	Katerini	Spain	Cornella de Llobregat	Spain	Sagunto	Italy	Pisa		
Greece	Serres	Spain	Majadahonda	Spain	Valdemoro	Italy	Massa		
Greece	Trikala	Spain	Torremolinos	Spain	Paterna	Italy	Cosenza		
Spain	Madrid	Spain	Castelldefels	Spain	Igualada	Italy	Savona		
Spain	Barcelona	Spain	Granollers	Spain	Torrent	Italy	Matera		
Spain	Valencia	Spain	Elda	Spain	Mislata	Italy	Acireale		
Spain	Sevilla	Spain	Mollet del Valles	Spain	Rivas-Vaciamadrid	Italy	Avellino		
Spain	Zaragoza	Spain	Granada	Spain	Esplugues de Llobregat	Italy	Altamura		

Spain	Malaga	Spain	Badalona	Spain	San Vicente del Raspeig	Italy	Bitonto		
Spain	Murcia	Spain	Mostoles	France	Montpellier	Italy	Molfetta		
Spain	Valladolid	Spain	Elche/Elx	France	Ajaccio	Italy	Battipaglia		
Spain	Palma de Mallorca	Spain	Cartagena	France	Toulon	Italy	Bisceglie		
Spain	Vitoria/Gasteiz	Spain	Sabadell	France	Avignon	Italy	Cerignola		
Spain	Pamplona	Spain	Jerez de la Frontera	France	Perpignan	Italy	Gela		
Spain	Toledo	Spain	Fuenlabrada	France	Nimes	Italy	Bagheria		
Spain	Badajoz	Spain	Alcala de Henares	France	Beziers	Italy	Anzio		
Spain	Logroño	Spain	Terrassa	France	Frejus	Italy	Messina		
Spain	Cordoba	Spain	Leganes	France	Aubagne	Italy	Prato		
Spain	Alicante/Alacant	Spain	Almeria	France	Aix-en-Provence	Italy	Livorno		
Spain	L'Hospitalet de Llobregat	Spain	Burgos	France	Marseille	Italy	Siracusa		
Spain	Reus	Spain	Salamanca	France	Nice	Italy	Latina		
Spain	Parla	Spain	Alcorcon	France	CA de Sophia-Antipolis	Italy	Terni		
Spain	San Fernando	Spain	Getafe	France	Valence	Italy	Giugliano in Campania		
Spain	Girona	Spain	Albacete	France	Martigues	Italy	Grosseto		
Spain	Caceres	Spain	Castellon de la Plana	France	Cannes	Italy	Brindisi		
Spain	Torrevieja	Spain	Huelva	Croatia	Rijeka	Italy	Trapani		
Spain	Pozuelo de Alarcon	Spain	Cadiz	Croatia	Split	Italy	Ragusa		
Spain	Puerto de Santa Maria, El	Spain	Leon	Croatia	Pula - Pola	Italy	Andria		
Spain	Coslada	Spain	Tarragona	Croatia	Zadar	Italy	Trani		
Spain	Talavera de la Reina	Spain	Santa Coloma de Gramenet	Italy	Roma	Italy	L'Aquila		
Spain	Palencia	Spain	Jaen	Italy	Napoli	Portugal	Lisboa		
Spain	Sant Boi de Llobregat	Spain	Lleida	Italy	Palermo	Portugal	Coimbra		
Spain	Gandia	Spain	Ourense	Italy	Genova	Portugal	Setubal		
Spain	Rozas de Madrid, Las	Spain	Mataro	Italy	Firenze	Portugal	Aveiro		

Spain	Guadalajara	Spain	Dos Hermanas	Italy	Bari	Portugal	Faro		
Spain	Sant Cugat del Valles	Spain	Algeciras	Italy	Catania	Portugal	Seixal		
Spain	Manresa	Spain	Marbella	Italy	Perugia	Portugal	Amadora		

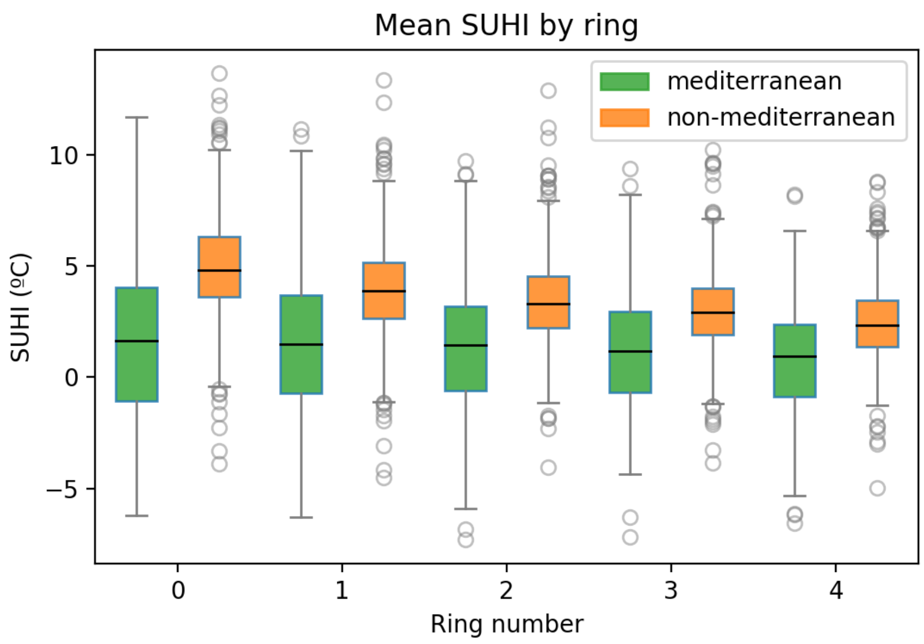

Figure S15. *Mean SUHI by ring for Mediterranean and non-Mediterranean cities.*

Table S16. *Kruskal-Wallis test results for SUHI differences in Mediterranean vs. non-Mediterranean cities.*

Kruskal-Wallis test (SUHI intensity)	
Ring	**p-value**
0	< 0.001 ***
1	< 0.001 ***
2	< 0.001 ***
3	< 0.001 ***
4	< 0.001 ***

** A non-parametric test was performed because the data did not comply with the homogeneity of variance assumption.*

Table S17. *Percentage of cities corresponding to each of the biomes for each urban configuration type.*

Urban configuration type	alpine	arctic	atlantic	black sea	boreal	continental	mediterranean	pannonian	steppic
Compact-High Density	3.3	0.4	6.9	0.8	0.4	45.5	36.2	3.7	2.9
Open Lowrise-Medium Density	1.2	0	50	0.4	0.8	27.5	17.2	2.9	0
Open Lowrise-Low Density	3.1	0	48.7	0	0	31.4	14.2	2.7	0
Green-Low Density	0	0	47.3	0	9.6	18.6	22.8	1.8	0

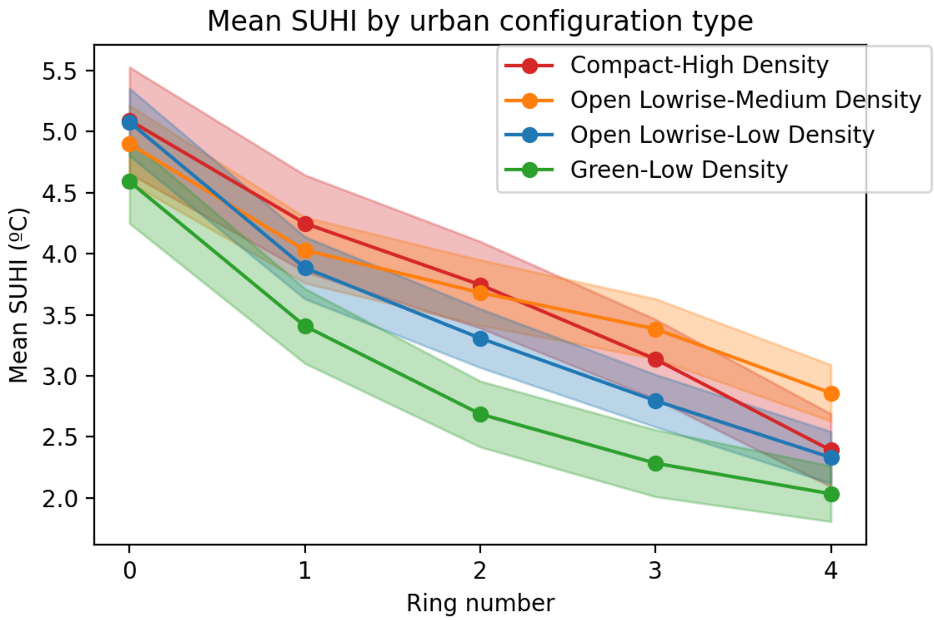

Figure S16. *SUHI intensity by urban configuration type excluding the Mediterranean cities. The mean and 95% CIs are shown.*

Table S18. *SUHI intensity by urban configuration type excluding the Mediterranean cities.*

		Compact-High Density			Open Lowrise-Medium Density			Open Lowrise-Low Density			Green-Low Density		
Variable	Level	**Mean (SE)**	**95% CI**		**Mean (SE)**	**95% CI**		**Mean (SE)**	**95% CI**		**Mean (SE)**	**95% CI**	
SUHI (ºC)	City	3.7 (0.1)	3.5	3.9	3.8 (0.1)	3.6	3.9	3.5 (0.1)	3.4	3.6	3 (0.1)	2.9	3.1
	Ring 0	5.1 (0.2)	4.7	5.5	4.9 (0.2)	4.6	5.2	5.1 (0.1)	4.8	5.4	4.6 (0.2)	4.2	4.9
	Ring 1	4.2 (0.2)	3.9	4.6	4 (0.1)	3.8	4.3	3.9 (0.1)	3.6	4.1	3.4 (0.2)	3.1	3.7
	Ring 2	3.7 (0.2)	3.4	4.1	3.7 (0.1)	3.4	3.9	3.3 (0.1)	3.1	3.5	2.7 (0.1)	2.4	3
	Ring 3	3.1 (0.2)	2.8	3.5	3.4 (0.1)	3.1	3.6	2.8 (0.1)	2.6	3	2.3 (0.1)	2	2.6
	Ring 4	2.4 (0.2)	2.1	2.7	2.9 (0.1)	2.6	3.1	2.3 (0.1)	2.1	2.5	2 (0.1)	1.8	2.3

Table S19. *Dunn's test results for the SUHI intensity excluding the Mediterranean cities.*

	Dunn's test (SUHI intensity)		
Ring	**Compared urban configuration types**		**p-value**
0	Compact-High Density	Open Lowrise-Medium Density	0.59
	Compact-High Density	Open Lowrise-Low Density	0.99
	Compact-High Density	Green-Low Density	0.01 *
	Open Lowrise-Medium Density	Open Lowrise-Low Density	0.57
	Open Lowrise-Medium Density	Green-Low Density	0.03 *
	Open Lowrise-Low Density	Green-Low Density	0.008 **
1	Compact-High Density	Open Lowrise-Medium Density	0.61
	Compact-High Density	Open Lowrise-Low Density	0.10
	Compact-High Density	Green-Low Density	< 0.001 ***
	Open Lowrise-Medium Density	Open Lowrise-Low Density	0.22
	Open Lowrise-Medium Density	Green-Low Density	0.001 **
	Open Lowrise-Low Density	Green-Low Density	0.03 *
2	Compact-High Density	Open Lowrise-Medium Density	0.63
	Compact-High Density	Open Lowrise-Low Density	0.07
	Compact-High Density	Green-Low Density	< 0.001 ***
	Open Lowrise-Medium Density	Open Lowrise-Low Density	0.01 *
	Open Lowrise-Medium Density	Green-Low Density	< 0.001 ***
	Open Lowrise-Low Density	Green-Low Density	0.003 **
3	Compact-High Density	Open Lowrise-Medium Density	0.04 *
	Compact-High Density	Open Lowrise-Low Density	0.12
	Compact-High Density	Green-Low Density	< 0.001 ***
	Open Lowrise-Medium Density	Open Lowrise-Low Density	< 0.001 ***
	Open Lowrise-Medium Density	Green-Low Density	< 0.001 ***

	Open Lowrise-Low Density	Green-Low Density	0.01 *
4	Compact-High Density	Open Lowrise-Medium Density	0.001 **
	Compact-High Density	Open Lowrise-Low Density	0.86
	Compact-High Density	Green-Low Density	0.06
	Open Lowrise-Medium Density	Open Lowrise-Low Density	< 0.001 ***
	Open Lowrise-Medium Density	Green-Low Density	< 0.001 ***
	Open Lowrise-Low Density	Green-Low Density	0.06

ii) Alternative SUHI estimation.

We explored an alternative approach to calculate the SUHI intensity, namely the Simplified Urban Extent (SUE) algorithm developed by Chakraborty and Lee (32). In this approach, the SUHI is defined as the LST difference between urban and non-urban land uses within the same urban extent, rather than the LST difference with the adjacent rural area. Additionally, the dataset estimates are adjusted for elevation, by masking out rural pixels that have an elevation difference greater than 50m with the urban pixels. This definition allows us to isolate the influence of extrinsic factors that may affect rural area's LST, such as peri urban areas, elevation, proximity to water bodies, and climatological factors; however, this has limitations in providing an accurate measure of the excess heat resulting from anthropogenic modification of natural landscapes as it takes as reference green urban areas, which are predominantly non-natural (i.e. artificial) landscapes. Note that there are other differences between these and the main estimates, including the different resolutions (Landsat at 30m native resolution versus the 1000m native resolution of the MODIS (Moderate Resolution Imaging Spectroradiometer) LST estimates used for the SUE algorithm), different return periods (every 16 days for Landsat versus daily for MODIS), and differences in view angles (much wider range of view angles for MODIS compared to Landsat), all of which would impact the degree of spatial variability within cities.

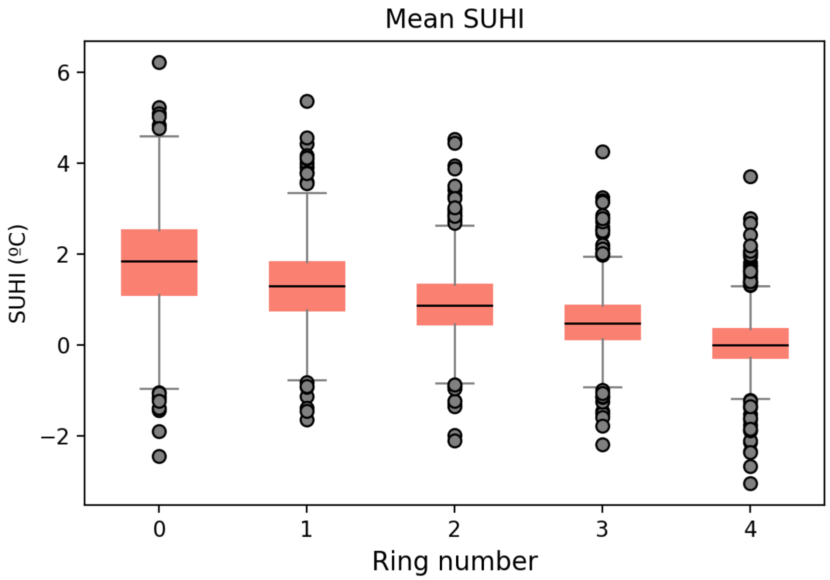

Figure S16. *Mean SUHI by ring considering an alternative approach for SUHI estimation.*

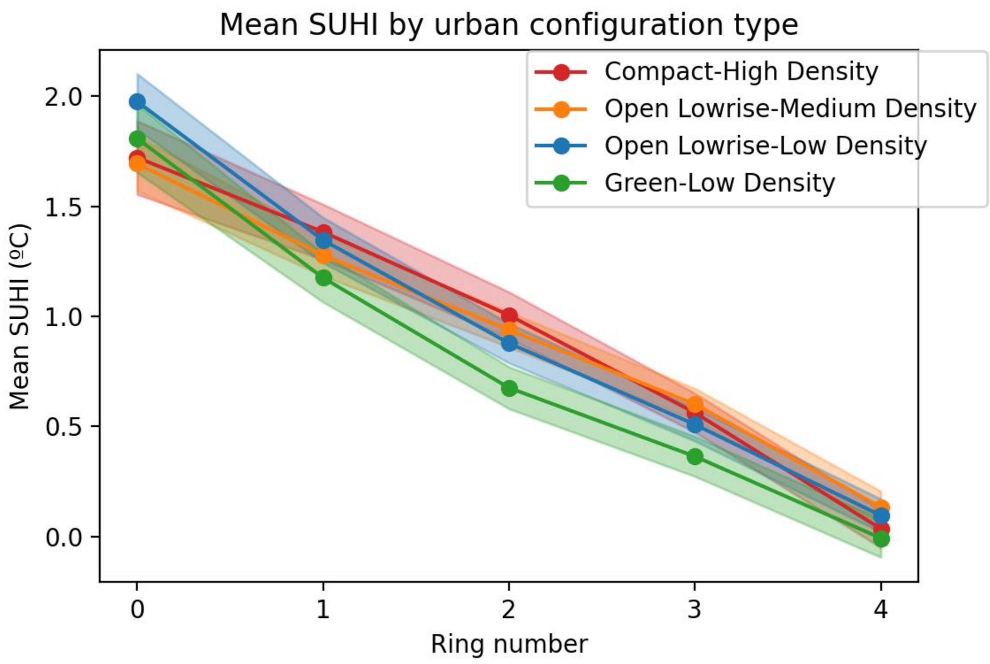

Figure S17. *SUHI intensity by urban configuration type using an alternative approach for SUHI estimation. The mean and 95% CIs are shown.*

Table S20. *SUHI intensity by urban configuration type using an alternative approach for SUHI estimation.*

		Compact-High Density			Open Lowrise-Medium Density			Open Lowrise-Low Density			Green-Low Density		
Variable	Level	**Mean (SE)**	**95% CI**		**Mean (SE)**	**95% CI**		**Mean (SE)**	**95% CI**		**Mean (SE)**	**95% CI**	
SUHI (ºC)	City	0.9 (0)	0.9	1	0.9 (0)	0.9	1	1 (0)	0.9	1	0.8 (0)	0.7	0.9
	Ring 0	1.7 (0.1)	1.6	1.9	1.7 (0.1)	1.6	1.8	2 (0.1)	1.8	2.1	1.8 (0.1)	1.7	2
	Ring 1	1.4 (0.1)	1.3	1.5	1.3 (0)	1.2	1.4	1.3 (0.1)	1.2	1.4	1.2 (0.1)	1.1	1.3
	Ring 2	1 (0.1)	0.9	1.1	0.9 (0)	0.9	1	0.9 (0)	0.8	1	0.7 (0)	0.6	0.8
	Ring 3	0.6 (0)	0.5	0.7	0.6 (0)	0.5	0.7	0.5 (0)	0.4	0.6	0.4 (0)	0.3	0.5
	Ring 4	0 (0)	0	0.1	0.1 (0)	0.1	0.2	0.1 (0)	0	0.2	0 (0)	-0.1	0.1

Table S21. *Dunn's test results for the SUHI intensity using an alternative approach for SUHI estimation.*

	Dunn's test (SUHI intensity)		
Ring	**Compared urban configuration types**		**p-value**
0	Compact-High Density	Open Lowrise-Medium Density	0.23
	Compact-High Density	Open Lowrise-Low Density	0.01 *
	Compact-High Density	Green-Low Density	0.23
	Open Lowrise-Medium Density	Open Lowrise-Low Density	< 0.001 ***
	Open Lowrise-Medium Density	Green-Low Density	0.04 *
	Open Lowrise-Low Density	Green-Low Density	0.31
1	Compact-High Density	Open Lowrise-Medium Density	0.04 *
	Compact-High Density	Open Lowrise-Low Density	0.47
	Compact-High Density	Green-Low Density	0.01 *
	Open Lowrise-Medium Density	Open Lowrise-Low Density	0.16
	Open Lowrise-Medium Density	Green-Low Density	0.56
	Open Lowrise-Low Density	Green-Low Density	0.07
2	Compact-High Density	Open Lowrise-Medium Density	0.21
	Compact-High Density	Open Lowrise-Low Density	0.02 *
	Compact-High Density	Green-Low Density	< 0.001 ***
	Open Lowrise-Medium Density	Open Lowrise-Low Density	0.28
	Open Lowrise-Medium Density	Green-Low Density	< 0.001 ***
	Open Lowrise-Low Density	Green-Low Density	0.006 **
3	Compact-High Density	Open Lowrise-Medium Density	0.45
	Compact-High Density	Open Lowrise-Low Density	0.16
	Compact-High Density	Green-Low Density	< 0.001 ***
	Open Lowrise-Medium Density	Open Lowrise-Low Density	0.03 *
	Open Lowrise-Medium Density	Green-Low Density	< 0.001 ***

	Open Lowrise-Low Density	Green-Low Density	0.03 *
4	Compact-High Density	Open Lowrise-Medium Density	0.05
	Compact-High Density	Open Lowrise-Low Density	0.62
	Compact-High Density	Green-Low Density	0.55
	Open Lowrise-Medium Density	Open Lowrise-Low Density	0.14
	Open Lowrise-Medium Density	Green-Low Density	0.02 *
	Open Lowrise-Low Density	Green-Low Density	0.30

L) **Mortality rates.**

i) Natural-cause mortality.

Natural-cause mortality rates were retrieved at the city level from our previous studies on the health impacts of environmental exposures in European cities, estimated based on data from the Eurostat city database for 2015 (6,7) . Briefly, we retrieved the population and all-cause mortality distribution in 5-year age groups (for adults aged 20 and older) and excluded the proportion of external deaths in each age group (identified by ICD10 codes V01-Y89) from all-cause mortality counts to obtain age-specific natural-cause mortality rates. Afterwards, the age-specific mortality rates were employed to estimate the age-standardized mortality based on the European standard population (33).

Table S22. Dunn's test results for the age-standardized natural-cause mortality rates.

Dunn's test (natural-cause mortality)		
Compared urban configuration types		**p-value**
Compact-High Density	Open Lowrise-Medium Density	0.17
Compact-High Density	Open Lowrise-Low Density	0.05
Compact-High Density	Green-Low Density	< 0.001 ***
Open Lowrise-Medium Density	Open Lowrise-Low Density	0.58
Open Lowrise-Medium Density	Green-Low Density	< 0.001 ***
Open Lowrise-Low Density	Green-Low Density	< 0.001 ***

ii) Attributable mortality.

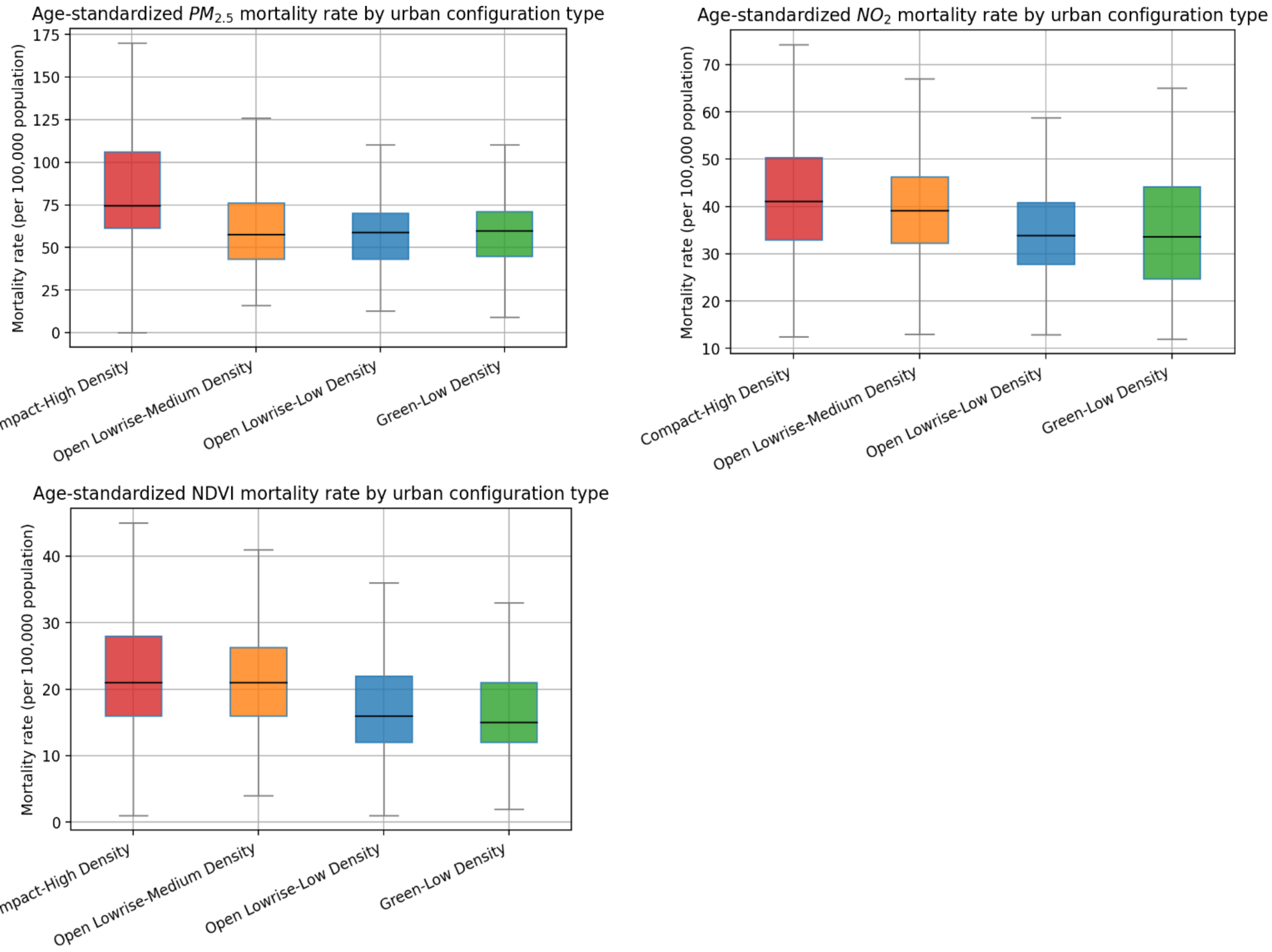

Figure S18. $PM_{2.5}$, NO_2 and lack of green space age-standardized attributable mortality rates by urban configuration type.

Table S23. $PM_{2.5}$, NO_2 and lack of green space age-standardized attributable mortality rates by urban configuration type.

	Compact-High Density			Open Lowrise-Medium Density			Open Lowrise-Low Density			Green-Low Density		
	Mean (SE)	95% CI		Mean (SE)	95% CI		Mean (SE)	95% CI		Mean (SE)	95% CI	
$PM_{2.5}$ attributable mortality (deaths per 100,000 inhabitants)	86 (2.3)	81	90	62 (1.7)	59	66	63 (1.9)	60	67	61 (2.3)	56	65
NO_2 attributable mortality (deaths per 100,000 inhabitants)	42 (0.8)	41	44	40 (0.7)	38	41	34 (0.6)	33	36	35 (1)	33	37
NDVI attributable mortality (deaths per 100,000 inhabitants)	22 (0.7)	21	23	22 (0.6)	20	23	17 (0.5)	16	18	17 (0.6)	16	18

** NDVI: Normalized Difference Vegetation Index*

*** Data from Khomenko et al., 2021, Barboza et al., 2021.*

Table S24. Dunn's test results for the $PM_{2.5}$, NO_2 and lack of green space age-standardized attributable mortality rates.

Dunn's test ($PM_{2.5}$ mortality)		
Compared urban configuration types		**p-value**
Compact-High Density	Open Lowrise-Medium Density	< 0.001 ***
Compact-High Density	Open Lowrise-Low Density	< 0.001 ***
Compact-High Density	Green-Low Density	< 0.001 ***
Open Lowrise-Medium Density	Open Lowrise-Low Density	0.68
Open Lowrise-Medium Density	Green-Low Density	0.76
Open Lowrise-Low Density	Green-Low Density	0.94
Dunn's test ($NO_{2.}$ mortality)		
Compared urban configuration types		**p-value**
Compact-High Density	Open Lowrise-Medium Density	0.04 *
Compact-High Density	Open Lowrise-Low Density	< 0.001 ***
Compact-High Density	Green-Low Density	< 0.001 ***
Open Lowrise-Medium Density	Open Lowrise-Low Density	< 0.001 ***
Open Lowrise-Medium Density	Green-Low Density	< 0.001 ***
Open Lowrise-Low Density	Green-Low Density	0.66
Dunn's test (NDVI mortality)		
Compared urban configuration types		**p-value**
Compact-High Density	Open Lowrise-Medium Density	0.84
Compact-High Density	Open Lowrise-Low Density	< 0.001 ***
Compact-High Density	Green-Low Density	< 0.001 ***

Open Lowrise-Medium Density	Open Lowrise-Low Density	< 0.001 ***
Open Lowrise-Medium Density	Green-Low Density	< 0.001 ***
Open Lowrise-Low Density	Green-Low Density	0.41

REFERENCES

1. Eurostat. Urban Audit [Internet]. 2018. Available from: https://ec.europa.eu/eurostat/web/gisco/geodata/reference-data/administrative-units-statistical-units/urban-audit

2. Dijkstra L, Poelman H. Cities in Europe. The new OECD-EC definition. [Internet]. 2012. Available from: https://ec.europa.eu/regional_policy/en/information/publications/regional-focus/2012/cities-in-europe-the-new-oecd-ec-definition

3. Office for National Statistics. How the population changed in the City of London: Census 2021 [Internet]. 2022. Available from: https://www.ons.gov.uk/visualisations/censuspopulationchange/E09000001/

4. European Commission. Global Human Settlement [Internet]. 2019. Available from: https://ghsl.jrc.ec.europa.eu/data.php

5. Iungman T, Cirach M, Marando F, Barboza EP, Khomenko S, Masselot P, et al. Cooling cities through urban green infrastructure: a health impact assessment of European cities. Lancet. 2023;401(10376):577–89.

6. Pereira-Barboza E, Cirach M, Khomenko S, Iungman T, Mueller N, Barrera-Gómez J, et al. Green space and mortality in European cities: a health impact assessment study. Lancet Planet Heal. 2021;5(10):e718–30.

7. Khomenko S, Cirach M, Pereira-Barboza E, Mueller N, Barrera-Gómez J, Rojas-Rueda D, et al. Premature mortality due to air pollution in European cities: a health impact assessment. Lancet Planet Heal. 2021;5(3):e121–34.

8. Khomenko S, Cirach M, Barrera-Gómez J, Pereira-Barboza E, Iungman T, Mueller N, et al. Impact of road traffic noise on annoyance and preventable mortality in European cities: A health impact assessment. Environ Int. 2022;162:107160.

9. Demuzere M, Bechtel B, Middel A, Mills G. Mapping Europe into local climate zones. PLoS One. 2019;14(4):e0214474.

10. Demuzere M, Bechtel B, Middel A, Mills G. European LCZ map [Internet]. 2020. Available from: 10.6084/m9.figshare.13322450

11. OpenStreetMap contributors. Planet OSM [Internet]. 2015. Available from: https://www.openstreetmap.org/

12. U.S. Geological Survey. Landsat-8, Collection 2, Level-2 [Internet]. 2023. Available from: https://www.usgs.gov/landsat-missions/landsat-data-access

13. Copernicus Land Monitoring Service. Corine Land Cover (CLC) 2018 (Version 2020_20u1) [Internet]. 2018. Available from: https://land.copernicus.eu/pan-european/corine-land-cover

14. Copernicus. Climate variables for cities in Europe from 2008 to 2017 [Internet]. 2019. Available from: https://cds.climate.copernicus.eu/cdsapp#!/dataset/sis-urban-climate-cities?tab=overview

15. Pérez-Invernón FJ, Huntrieser H, Erbertseder T, Loyola D, Valks P, Liu S, et al. Quantification of lightning-produced NOx over the Pyrenees and the Ebro Valley by using different TROPOMI-NO2 and cloud research products. Atmos Meas Tech. 2022;15(11):3329–51.

16. Lu X, Ye X, Zhou M, Zhao Y, Weng H, Kong H, et al. The underappreciated role of agricultural soil nitrogen oxide emissions in ozone pollution regulation in North China. Nat Commun. 2021;12:5021.

17. Voigt C, Lelieveld J, Schlager H, Schneider J, Curtius J, Meerkötter R, et al. Cleaner Skies during the COVID-19 Lockdown. Bull Am Meteorol Soc. 2022;103(8):E1796–E1827.

18. Müller I, Erbertseder T, Taubenböck H. Tropospheric NO2: Explorative analyses of spatial variability and impact factors. Remote Sens Environ. 2022;270(2):112839.

19. Erbertseder T, Hannes Taubenböck TE, Gilardi L, Paeth H, Marconcini M, Dech S. Earth Observation-based analysis of NO2 pollution and settlement growth in megacities. In: 2023 Joint Urban Remote Sensing Event (JURSE) [Internet]. 2023. Available from: 10.1109/JURSE57346.2023.10144190

20. Samad A, Kiseleva O, Holst CC, Wegener R, Kossmann M, Meusel G, et al. Meteorological and air quality measurements in a city region with complex terrain: influence of meteorological phenomena on urban climate. Meteorol Zeitschrift. 2023;

21. Veefkind JP, Aben I, McMullan K, Förster H, Vries J de, Otter G, et al. TROPOMI on the ESA Sentinel-5 Precursor: A GMES mission for global observations of the atmospheric composition for climate, air quality and ozone layer applications. Remote Sens Environ. 2012;120:70–83.

22. Geffen J van, Boersma KF, Eskes H, Sneep M, Linden M ter, Zara M, et al. S5P TROPOMI NO2 slant column retrieval: method, stability, uncertainties and comparisons with OMI. Atmos Meas Tech. 2020;13(3):1315–35.

23. Goldberg DL, Anenberg SC, Kerr GH, Mohegh A, Lu Z, Streets DG. TROPOMI NO2 in the United States: A Detailed Look at the Annual Averages, Weekly Cycles, Effects of Temperature, and Correlation With Surface NO2Concentrations. Earth's Futur. 2021;9(4):e2020EF001665.

24. Oda T, Maksyutov S, Andres RJ. The Open-source Data Inventory for Anthropogenic CO2, version 2016 (ODIAC2016): a global monthly fossil fuel CO2 gridded emissions data product for tracer transport simulations and surface flux inversions. Earth Syst Sci Data. 2018;10:87–107.

25. McInnes L, Healy J, Melville J. UMAP: Uniform Manifold Approximation and Projection for Dimension Reduction [Internet]. 2018. Available from: https://umap-learn.readthedocs.io/en/latest/index.html

26. McInnes L, Healy J, Melville J. UMAP: Uniform Manifold Approximation and Projection for Dimension Reduction. 2020; Available from: http://arxiv.org/abs/1802.03426

27. Coenen A, Adam P. Understanding UMAP [Internet]. 2023. Available from: https://pair-code.github.io/understanding-umap/

28. Amazon Web Services - Labs. On the Validation of UMAP [Internet]. 2022. Available from: https://github.com/awslabs/amazon-denseclus/blob/main/notebooks/Validation For UMAP.ipynb

29. Kuenen J, Dellaert S, Visschedijk A, Jalkanen JP, Super I, Denier Van Der Gon H. CAMS-REG-v4: a state-of-the-art high-resolution European emission inventory for air quality modelling. Earth Syst Sci Data. 2022;14(2):491–515.

30. ECCAD. Emissions of atmospheric Compounds and Compilation of Ancillary Data [Internet]. 2022. Available from: https://eccad.aeris-data.fr/

31. European Environment Agency. Air Quality e-Reporting (AQ e-Reporting) [Internet]. 2022. Available from: https://www.eea.europa.eu/en/datahub/datahubitem-view/3b390c9c-f321-490a-b25a-ae93b2ed80c1

32. Chakraborty T, Lee X. A simplified urban-extent algorithm to characterize surface urban heat islands on a global scale and examine vegetation control on their spatiotemporal variability. Int J Appl Earth Obs Geoinf. 2019;74:269–80.

33. Eurostat. Revision of the European Standard Population. Report of Eurostat's task force. [Internet]. 2013. Available from: https://ec.europa.eu/eurostat/web/products-manuals-and-guidelines/-/ks-ra-13-028